VHP Male CAD Mesh Processing for MRI Testing

A Major Qualifying Project Report
Submitted to the Faculty
of the
WORCESTER POLYTECHNIC INSTITUTE
in partial fulfillment of the requirements for the
Degree of Bachelor of Science
in Electrical and Computer Engineering

By

Mizael Soto

Submitted to Professor Sergey Makarov

April 26, 2018

Abstract

The purpose of this MQP was to aid in creating high quality Male Human Body Computer-Aided Design (CAD) Models for Finite Element Method analysis. These CAD models can be used to run multiple real world simulation cases that would benefit research in multiple fields. The CAD meshes that have been processed for this MQP will be used for MRI and electromagnetic simulations. During the execution of this MQP, a workflow was developed to assist in processing these CAD meshes at a high rate, with a low number of triangles to enable faster analysis. At the same time, high quality triangular meshes were generated without losing major details of the physical structure.

Acknowledgements

I would like to express my gratitude to the following people and organizations for their support throughout the project process:

- Worcester Polytechnic Institute and the Electrical and Computer Engineering Department for giving me the opportunity to work on this project.
- Professor Sergey Makarov for advising the project and providing me with guidance and encouragement throughout the process.
- Doctor Greg Noetscher for his valuable inputs and feedback, which has helped me, to complete my work.

Table of Contents

Table of Figures

Table of Tables

Introduction

Virtual Humans

Virtual humans are three dimensional computer generated human models of actual physical people. These models are used to help simulate real world effects that certain applications may have on a human being, without the need to use a real human subject for testing. These models enable companies and researchers to conduct several thousands of experiments at a higher pace and in a way that maximizes human safety factors.

There are a variety of application that virtual human models are used by researchers to create and test several different types' of equipment through safe methods which are much faster than ever before. Prior to these model being used by researchers the models must be converted to high quality surface meshes that can be accurately processed through different computational software's for different applications. The models in this MQP are to be converted to triangular meshes to be used for MRI and electromagnetic simulations.

Visible Human Project

The Visible Human Project (VHP) was established by the U.S. National Library of Medicine in 1989. The goal behind VHP was to produce a complete three dimensional image dataset of the human male and female anatomy, which could be used as tools to study human anatomy. This dataset included digital images of both computed tomography (CT) and magnetic resonance images (MRI) from the cryosectioned cadavers. The datasets for both cadavers were released to the public starting with the male model in November 1994, and the female model in November 1995 [1].

The separation on both the male and female cadavers was accomplished in very similar ways. The process was started by first scanning the entire body via MRI and CT. The bodies where then frozen and cut into intervals of a certain sizes which were then individually photographed using a high resolution camera. The difference between the male and female datasets was in the spacing of the cuts that was used. The male cadaver was cut using 1 millimeter intervals, resulting in 1,871 slices and 15 gigabytes of data. The female cadaver was cut in 0.33 millimeter intervals, resulting in 5,189 slices and 40 gigabytes of data [2].

This dataset is an important tool that is used around the world every day for many different applications. These applications include but are not limited to: academic research, educational tools, mathematical analysis, and medical uses [1].

Computational Modeling

Computational modeling using these virtual humans combines fields of mathematics, physics, anatomy, and computer science to study the reactions and behaviors of complex biomedical problems. The National Institutes of Health points out that creating these models and using them in order to simulate real applications at such a high rate will most likely help researchers find solutions to current problems that are still being solved [3].

Computational human modeling has helped make great strides in industries and fields like biomedical research, automotive safety research, radiology, and electromagnetic research. As an example of how computational humans are used, consider some potential uses in electromagnetic studies. In these applications, computational humans are generally used to perform safety and performance evaluations for a variety of medical devices. Examples of such devices include electrophysiology monitoring devices, MRI systems, pacemakers, and stents [5].

Problem Statement

Although many computational models exist and have a wide variety of uses, the problem we encounter is with the composition of the models themselves. The vast majority of the virtual human models currently available are voxel models and not CAD models. Utilizing a CAD or voxel model is an important distinction. Depending on which type of model we use will affect the type of Computational Electromagnetics (CEM) problems that can be solved, and determines the electromagnetic solver type [5]. Voxel models are also not suitable for Finite Element Method (FEM) or Method of Moments (MOM) frequency domain analysis. Because of this, there is a large need for anatomically correct virtual human models that are compatible with FEM software.

Human Model Construction

Voxel models are usually created via a set of 3D mathematical algorithms commonly called image segmentation. To understand how it works, consider the body image in Figure 1a, which shows a cross-section of a human leg including the patella [5]. The complete stack of images continue in the Z-direction and the boundaries of the patella will be traced with a set of discrete points in the xy-plane creating a polygon. In the end result we will have a complete set of the patella's boundary in three different dimensions, which is given to us in a point cloud system as seen in Figure 1b [5]. The inner volume of the point cloud system is either empty or can be filled with a set of uniformly distributed inner nodes, which provides us with a volumetric voxel model of the tissue.

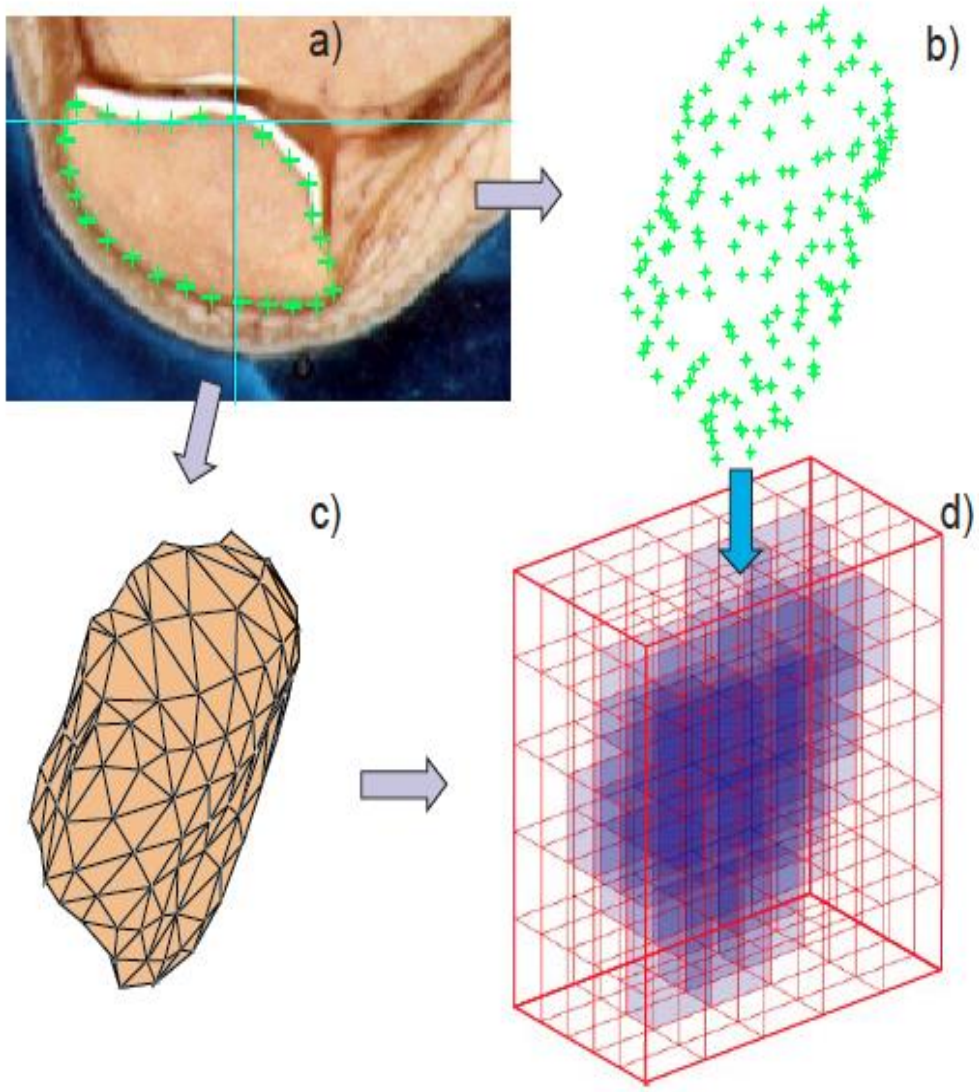

Figure 1. A- Image of a patella with traced boundary; B - Resulting point cloud; C- Patella CAD model; D- Patella voxel model

Mesh Processing

The goal of this MQP is in essence a continuation and extension of the 2017 "CAD Virtual Human Model" MQP project [7]. The difference between the two projects can be found in two distinct places. Like the previous project, voxel models of the virtual human 'AustinMan' [8] were taken and processed through a multistep process to create FEM suitable CAD models.

Due to the manner that voxel models are created, there is a need for suitable CAD models containing smooth, high quality triangular surfaces that can be used for simulation without errors due to the model itself. In addition, the development of a fast-paced compatible workflow was necessary to process and create high quality meshes for FEM analysis. While the human adult body is made up of roughly 206 bones, only 180 bone meshes were created due to the fact that certain neighboring bones were combined into one bone model for simplicity. Figure 2 below, is an example of a voxel bone model that serves as the starting point for this project.

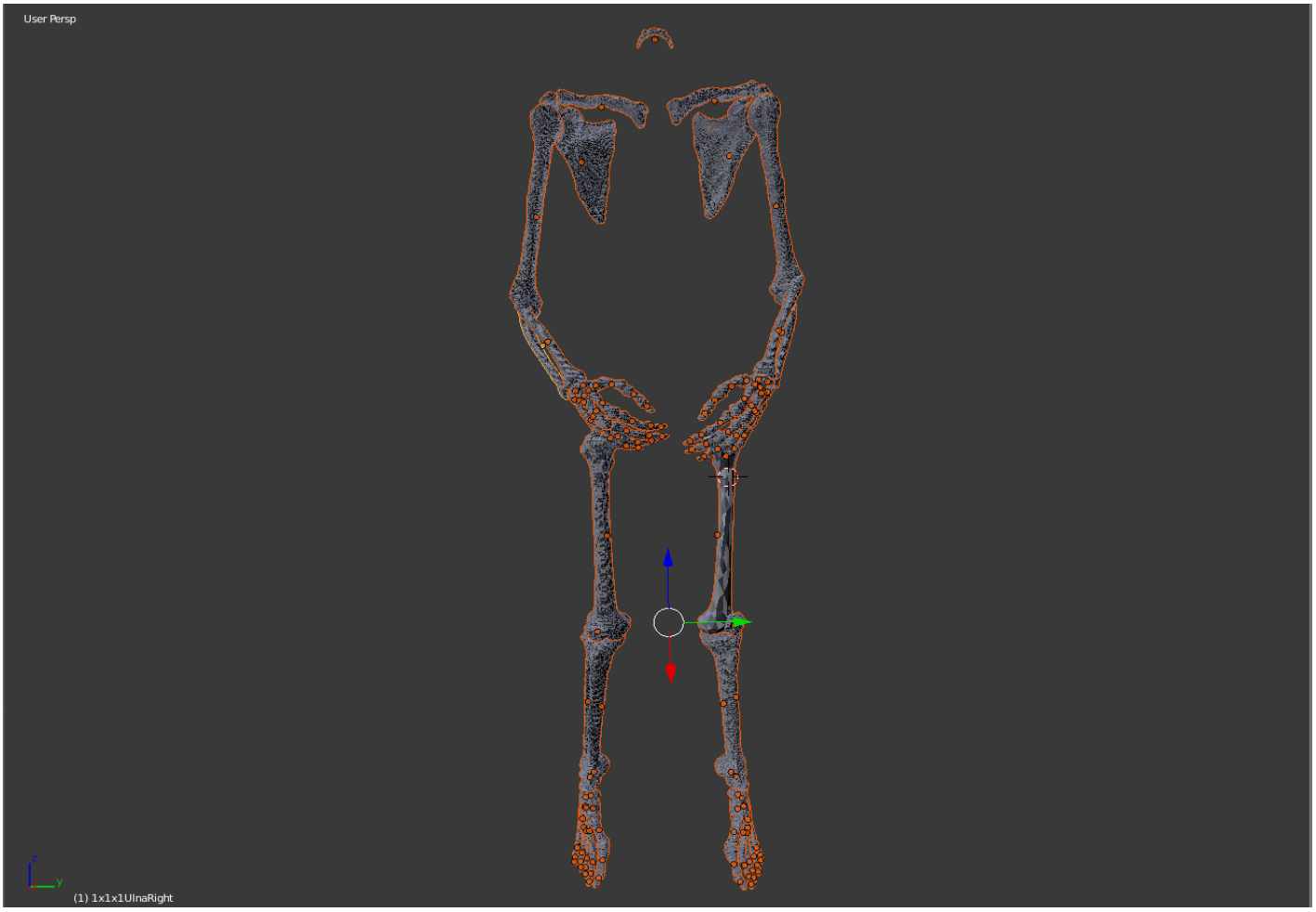

Figure 2. Voxel VHP male bone model Conditions for CAD models

For a CAD model to be considered of suitable quality to be used to accurately run FEM or MOM analysis, there are certain criteria that need to be met by the mesh itself. First, a CAD

mesh must be watertight. This means that the mesh must not contain any holes anywhere on its surface. Figure 3 serves as an example of what a non-watertight mesh would look like. Second a surface mesh must be well behaved all throughout and obey the manifold condition.

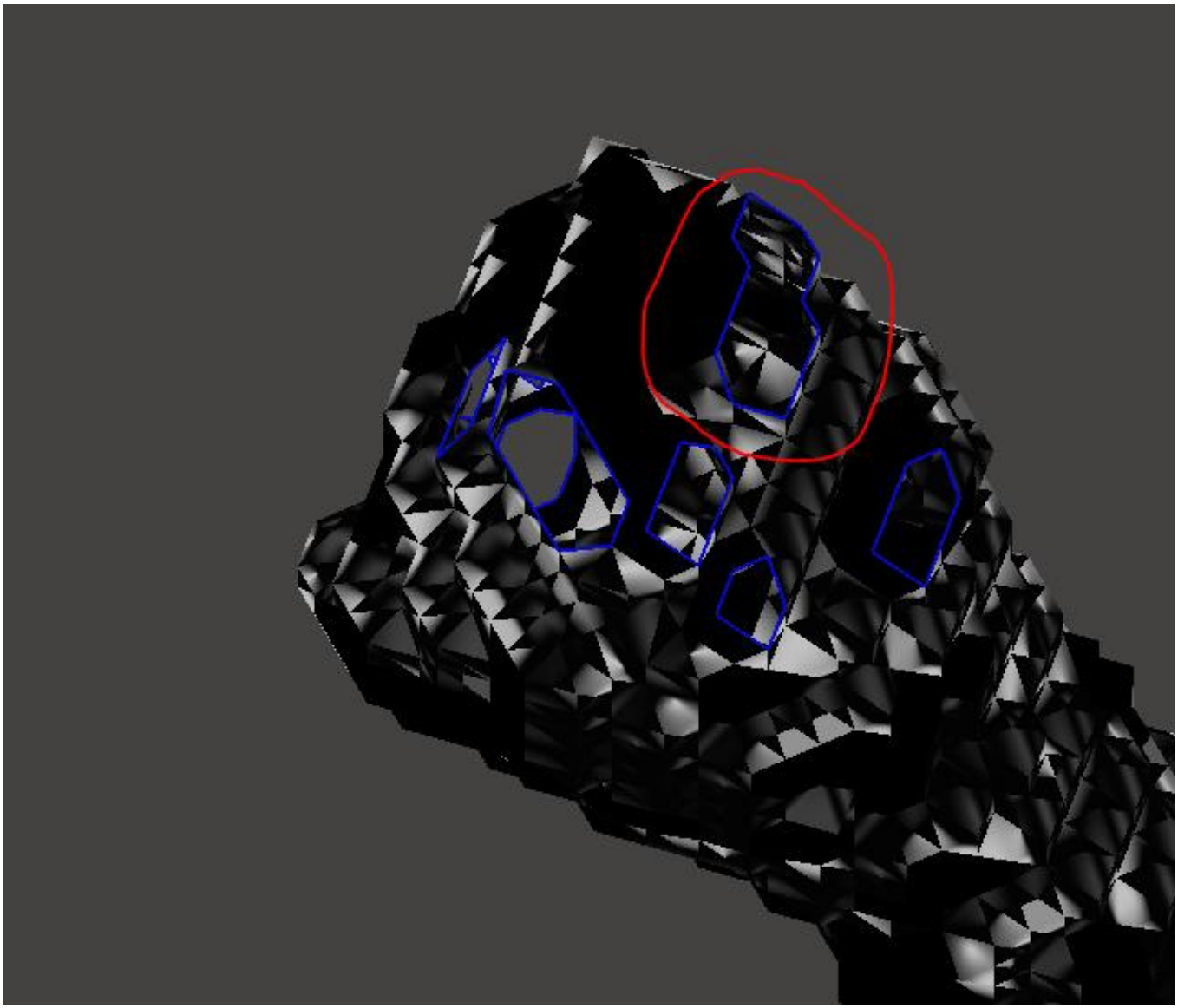

Figure 3. Unprocessed Right Fourth Metacarpal Bone Model with Holes

A mesh is considered 2-manifold if every node of the mesh has a disk-shaped neighborhood of triangles. Every edge of a 2-manifold mesh is a manifold edge with only two attached triangles.

Everything else is considered non-manifold and therefore not suitable for FEM analysis. A manifold edge is shown in Figure 4b; Figure 4c provides an example of a non-manifold edge.

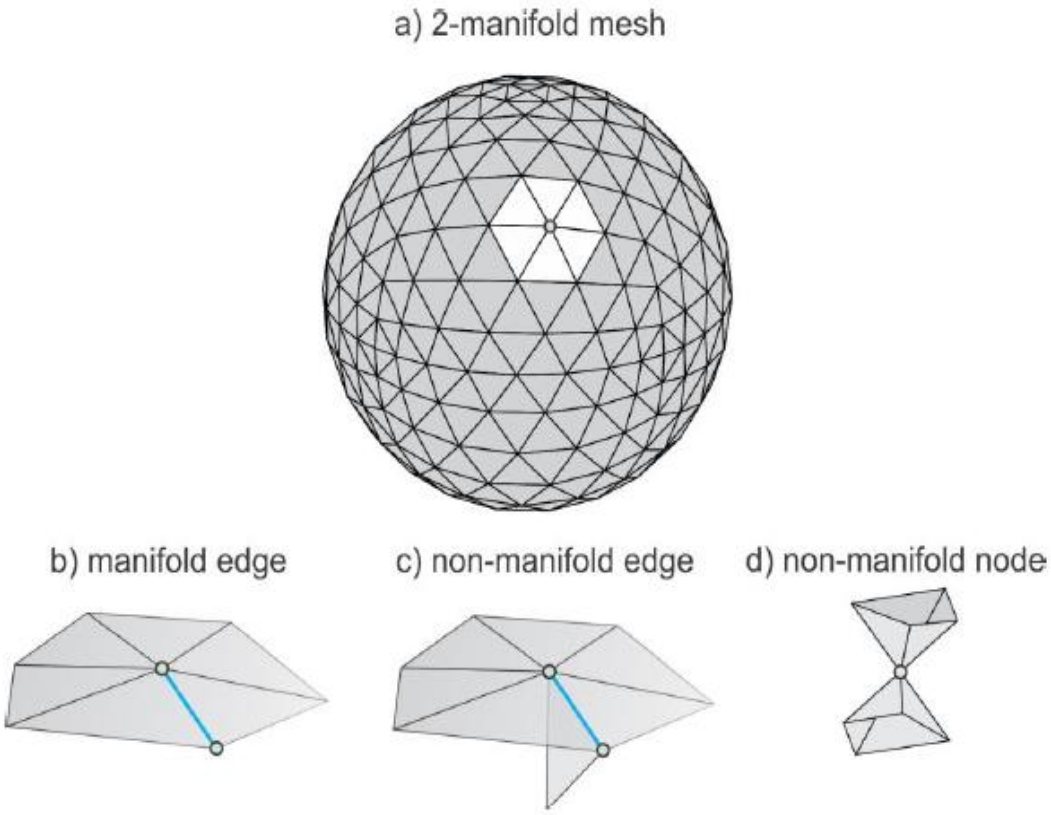

Figure 4. a) - A 2-manifold mesh; b) - Manifold edge; c) - Non-manifold edge; d) - Non-manifold node [6].

Additional Conditions for quality CAD Models

Considering the previous requirements for CAD models, there are some additional conditions that need to be considered prior to using a surface mesh for FEM analysis. The overall quality of the mesh itself is important to consider when constructing a CAD model for FEM analysis. Due to how voxel models are created the majority of meshes are generated through segmentation and then converted to a point cloud system so that we begin with a series of cubic regions, as shown in Figure 5.

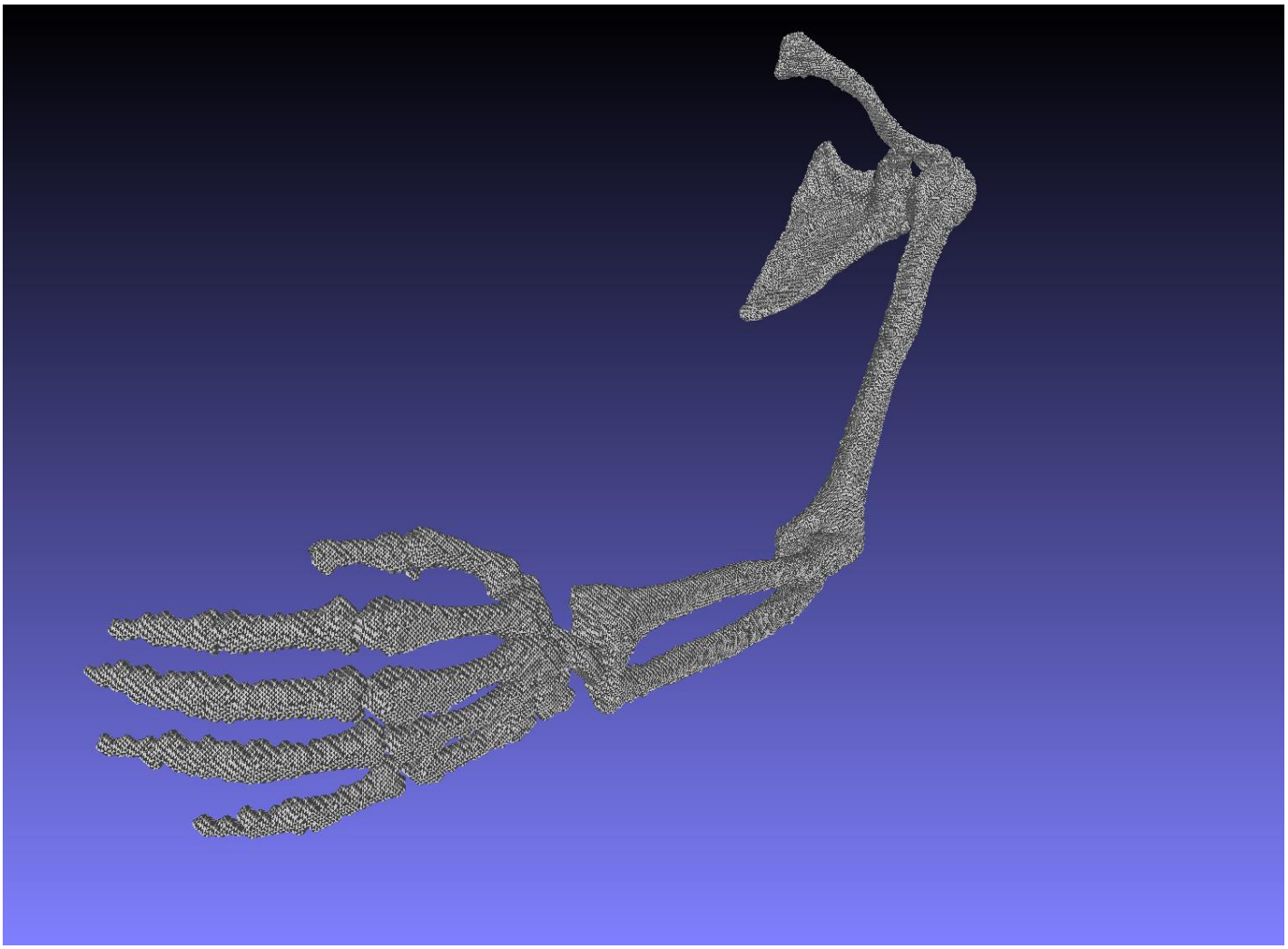

Figure 5. Close in view of voxel bone model left arm

These rigid non-smooth or pixelated models may provide a good representation of the tissue and bone samples, but are created with many cube-like structures that overlap and cause errors in the analysis. The next thing to consider is the number of triangles that are present on a surface mesh. The larger the number of triangles are, the longer it will take to process the mesh through FEM analysis. The last thing to consider when processing a mesh is the quality of each individual triangle on the mesh. The quality of the analysis and its results will depend on the quality of the mesh that it employs. The quality of a mesh can be described as the quality of your worst triangle present on the mesh. The quality of a triangle is a measure of the deviation from an equilateral

triangle, which is known as the best triangle in any mesh. One way to measure the quality of a triangle is seen in Figure 6, which is twice the ratio of the radius of the inscribed circle, donated as r_{in}, to the radius of the circumscribed circle r_{out}, or $q = \frac{2*r_{in}}{r_{out}}$.

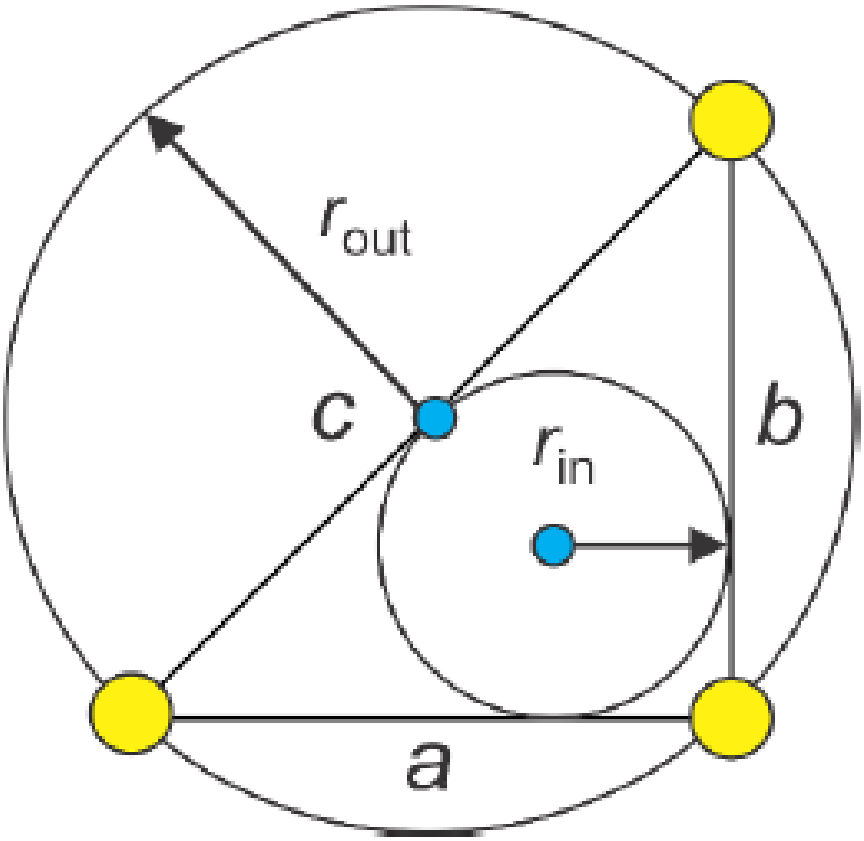

Figure 6. Triangle quality calculation model [6]

A value equal to or above 0.5 is considered good quality and is usually the target for the lowest quality triangle. Figure 7 shows an example of a bad quality triangles on a triangular mesh model.

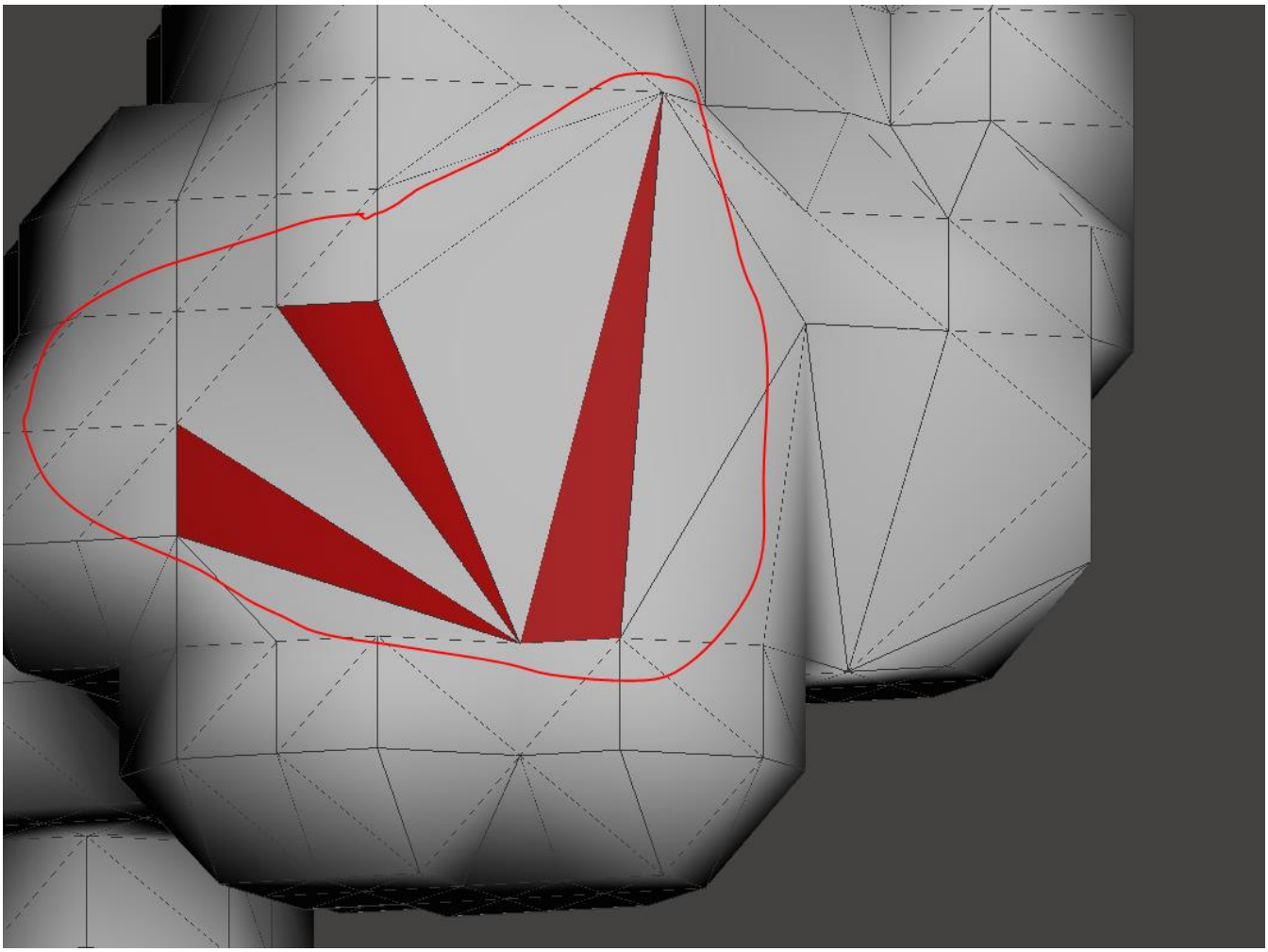

Figure 7. Zoomed in bad quality triangles on right hand phalange distal 3 mesh

Workflow

There are several different types of mesh processing software available, including Meshlab, Meshmixer, Blender, ANSYS, and SpaceClaim, among others. Each one has its strengths and weaknesses in terms of usability, resources, available tools and cost. In practice, the best way to process a mesh is to use a combination of these various mesh processing tools to achieve the goal of a good quality mesh. After careful consideration and much experimentation, a workflow was created to properly process meshes depending on the status and condition of the

mesh. Figure 8 displays a flow chart to follow when processing a mesh, and which mesh processing software will help you achieve your goal during a specific step.

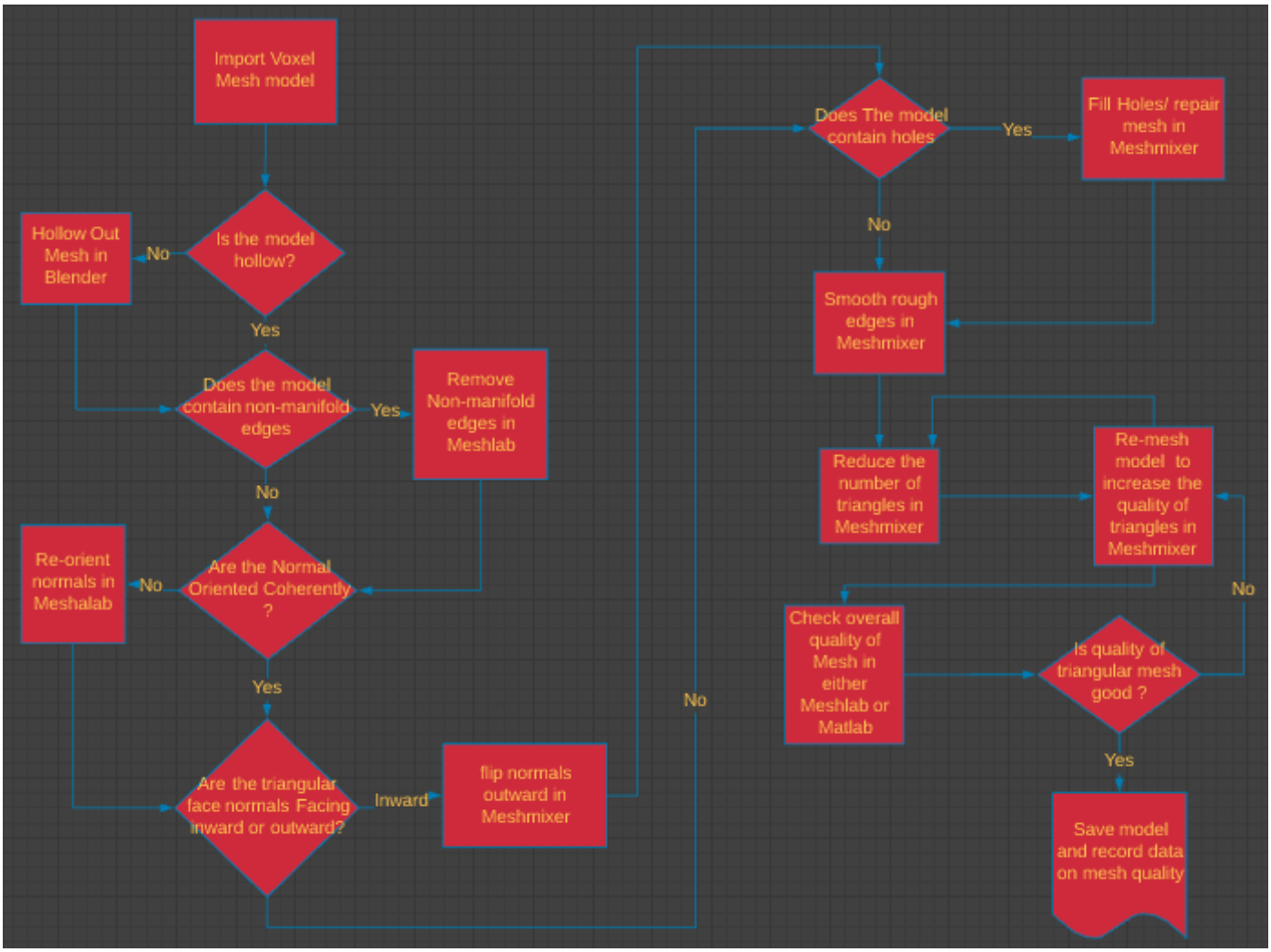

Figure 8. Mesh processing Flow chart

Hollowing

Referencing our flowchart from Figure 8, the first step in repairing a mesh is to check whether the model you are working on is hollow. As mentioned earlier due to the manner that the voxel models are created, there are occasions when some of the models we are processing have

not only an outer layer of mesh with distinct properties, but also an internal layer. To properly and accurately perform FEM analysis on a model, we need to make sure that only the outer surface layer of the mesh is being used. If other layers of triangular meshes exist, the analysis may be incorrect. Figure 9 is an example of a mesh that possess an additional internal layer that needs to go through a hollowing process.

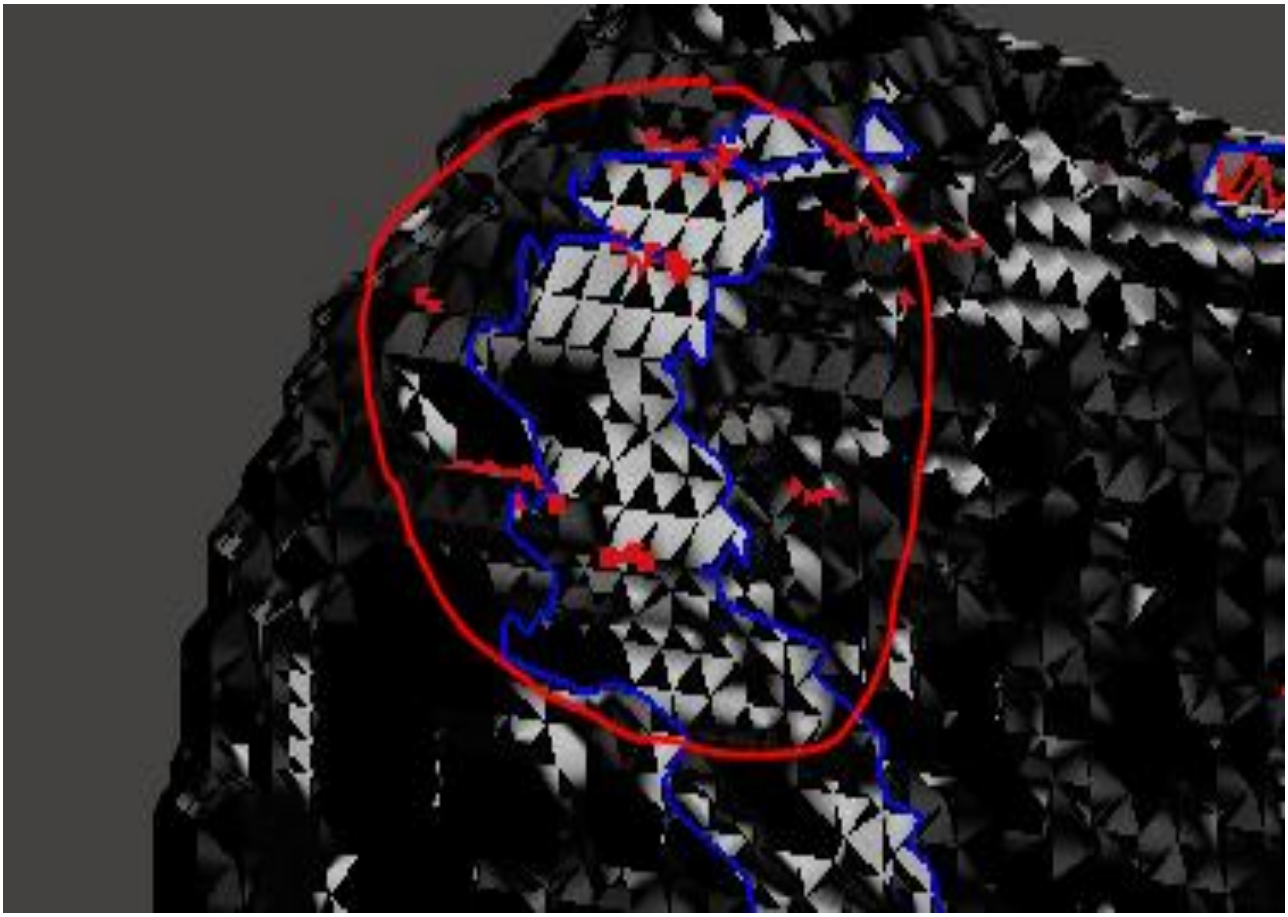

Figure 9. Zoomed in picture of a model that has an internal layer

The process is started by importing the model into the mesh processing software Blender. Once the model is imported into Blender you want to make sure that you set the origin of the scene to the imported model and then change the camera view to the model. If you attempt to move the model to the origin this will cause a translation of where the model exists in 3D space resulting in inconsistencies with the remaining model structures. Now that the model is in the view of our

scene, Blender has a specialized set of tools which enable us to not only tell whether the mesh needs to be hollowed out, but also employs a way to properly dispose of the inner layer without affecting the outer layer. Figure 10 displays Blender's wireframe mode, which enables us to see just the wireframe of our model.

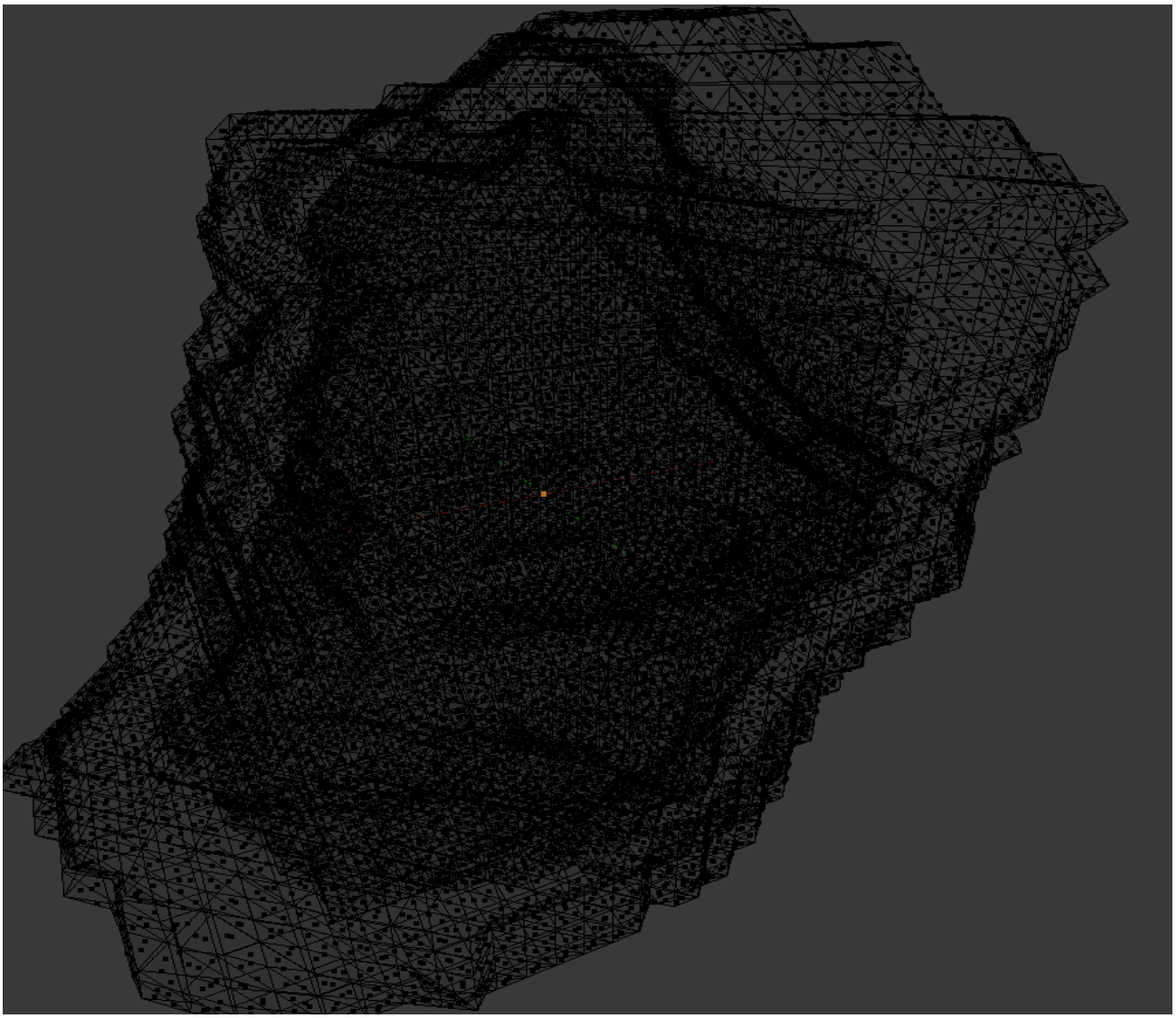

Figure 10. Blender wireframe tool used to spot internal mesh layers

If there is an internal component like the one shown in Figure 10, the next step is to remove the internal structure so that only the external surface mesh remains. This is accomplished within the

Blender environment by first turning off wireframe mode and enabling edit mode. In edit mode, you will be able to manipulate different properties of your model. With edit mode enabled and face select mode enabled, the next step is use the circle select tool within Blender to manually select all the external faces of the model as seen in Figure 11.

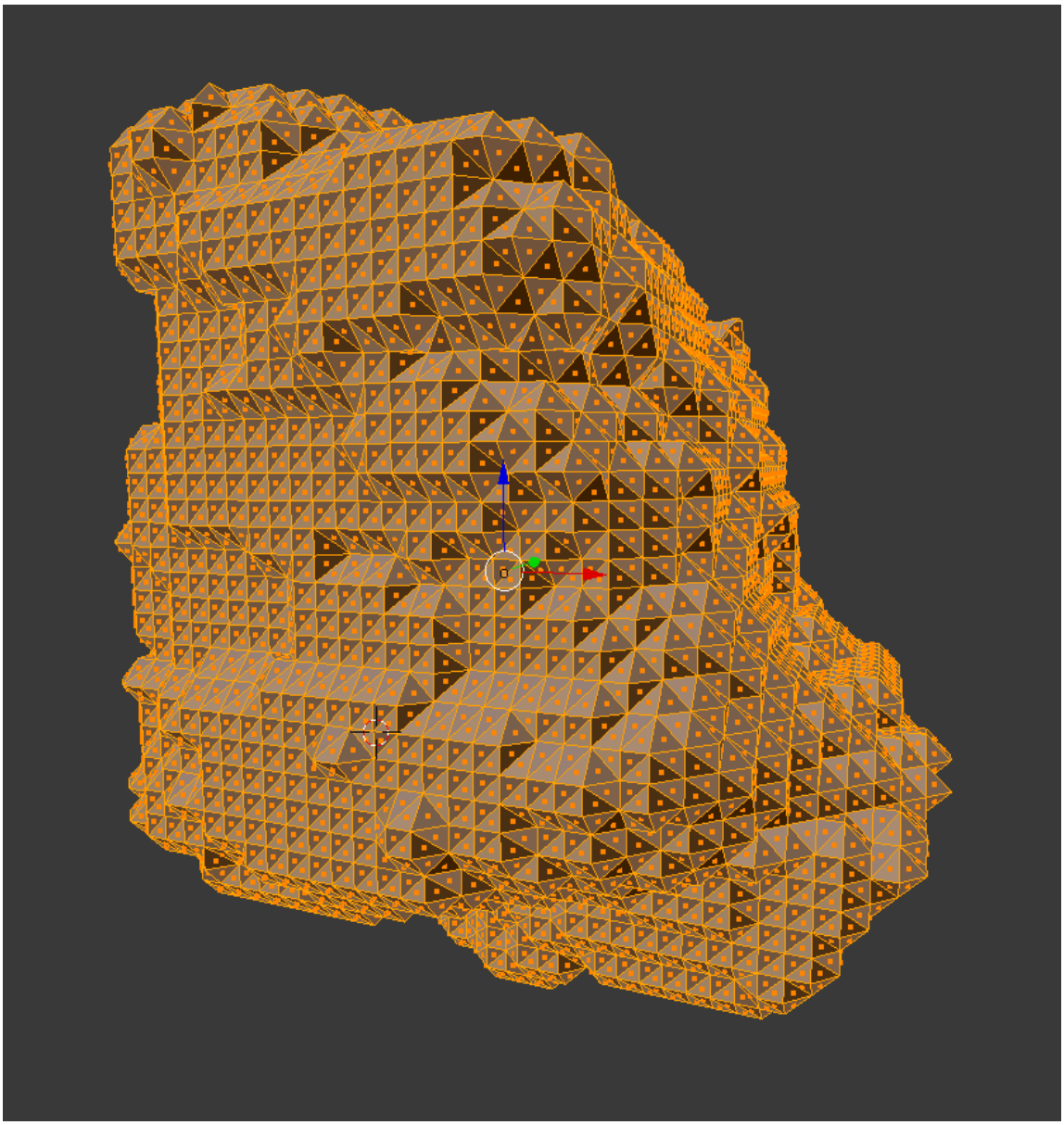

Figure 11. Selecting all external surface faces in Blender for hollowing process

When all the external triangular faces have been selected, the next step is to use the inverse select tool, which will select all the faces that are not currently selected; in this case, the internal faces

are selected and can be deleted. Now that those newly selected faces have been deleted, we have a model that only consists of triangles on the surface and none internally, as shown in Figure 12.

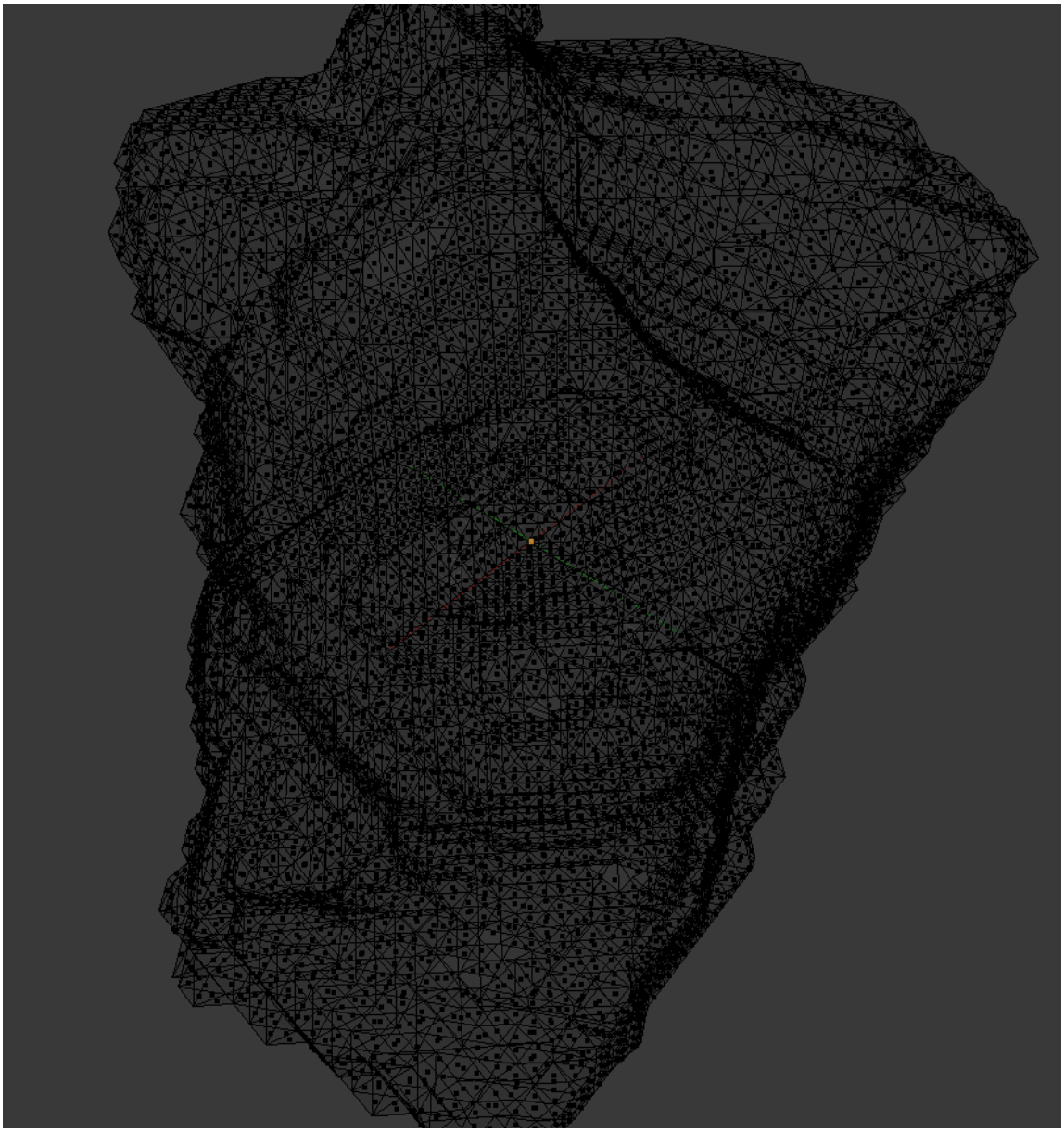

Figure 12. Hollowed surface mesh in Blender

The last part of this step is to make sure to export your now hollowed model. It is important to export it rather than save it due to the fact that saving it only allows us to use the new model within Blender. On the other hand if the model is exported you can choose the formatting style and the new model can then be used in a variety of other mesh processing software as necessary.

Removing Non-manifold edges and coherently aligning normals

The next two steps in the workflow are one of the most crucial ones which can affect all the future steps in properly fixing a model. These steps are to be done using the mesh processing software Meshlab instead of Blender. As mentioned earlier, a good triangular mesh is 2-manifold throughout the entire mesh surface. To check for non-manifold edges, first import the model into Meshlab. Meshlab has a tool that will locate and select any non-manifold edges, as can be seen in Figure 13. Then, using Meshlab's clean up tools, you can remove the faces from non-manifold edges to get rid of any self-intersecting faces causing non-manifold edges.

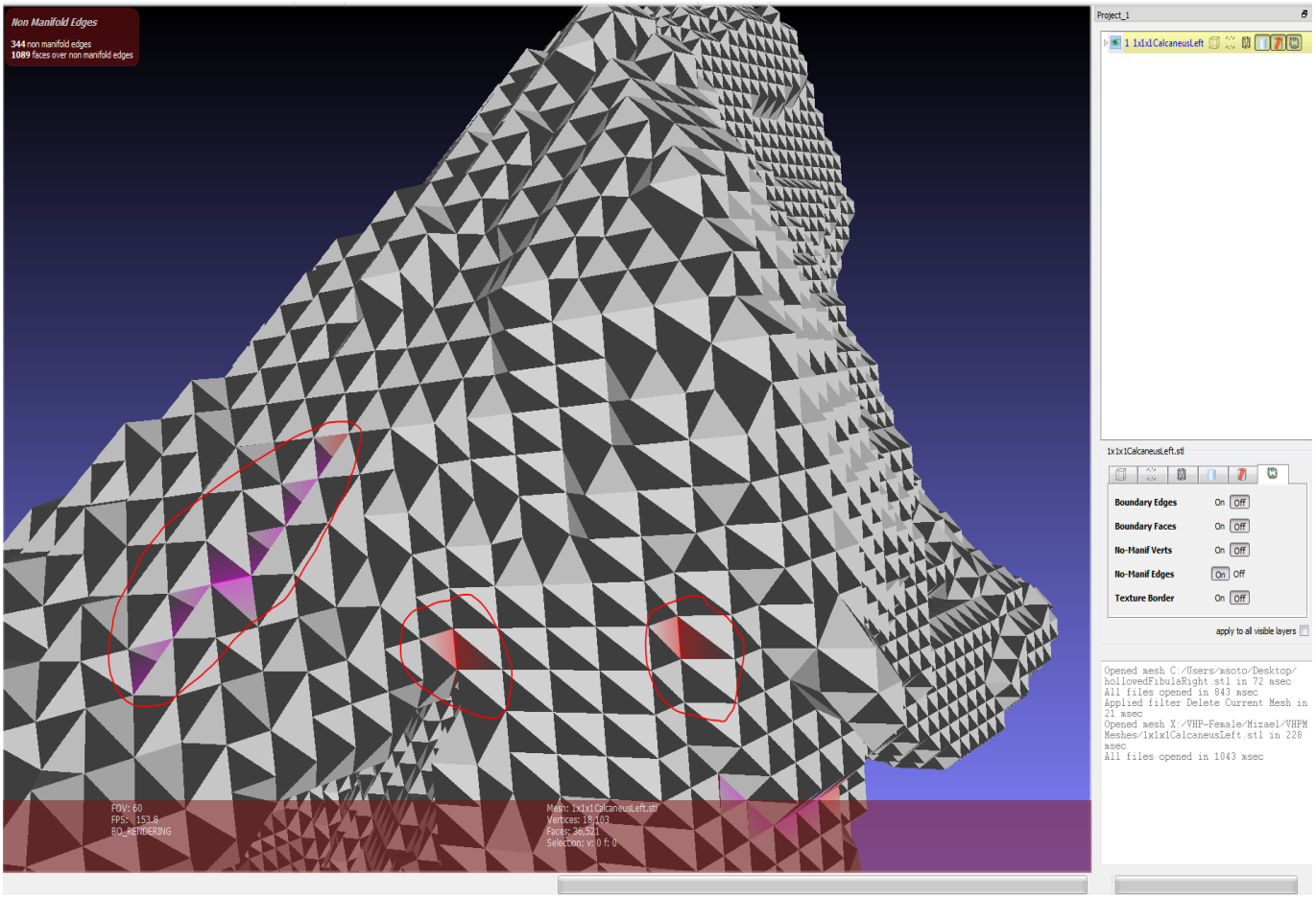

Figure 13. Displaying non-manifold edges in Meshlab

Once that is done, the next important step is to re-orient all the normal vectors of all triangular mesh faces such that they point in the same direction. This is necessary due to the fact that when voxel models are created out of cubes, all the normal planes of the triangular faces on the mesh are either facing inward or outward all throughout the mesh as seen in Figure 14.

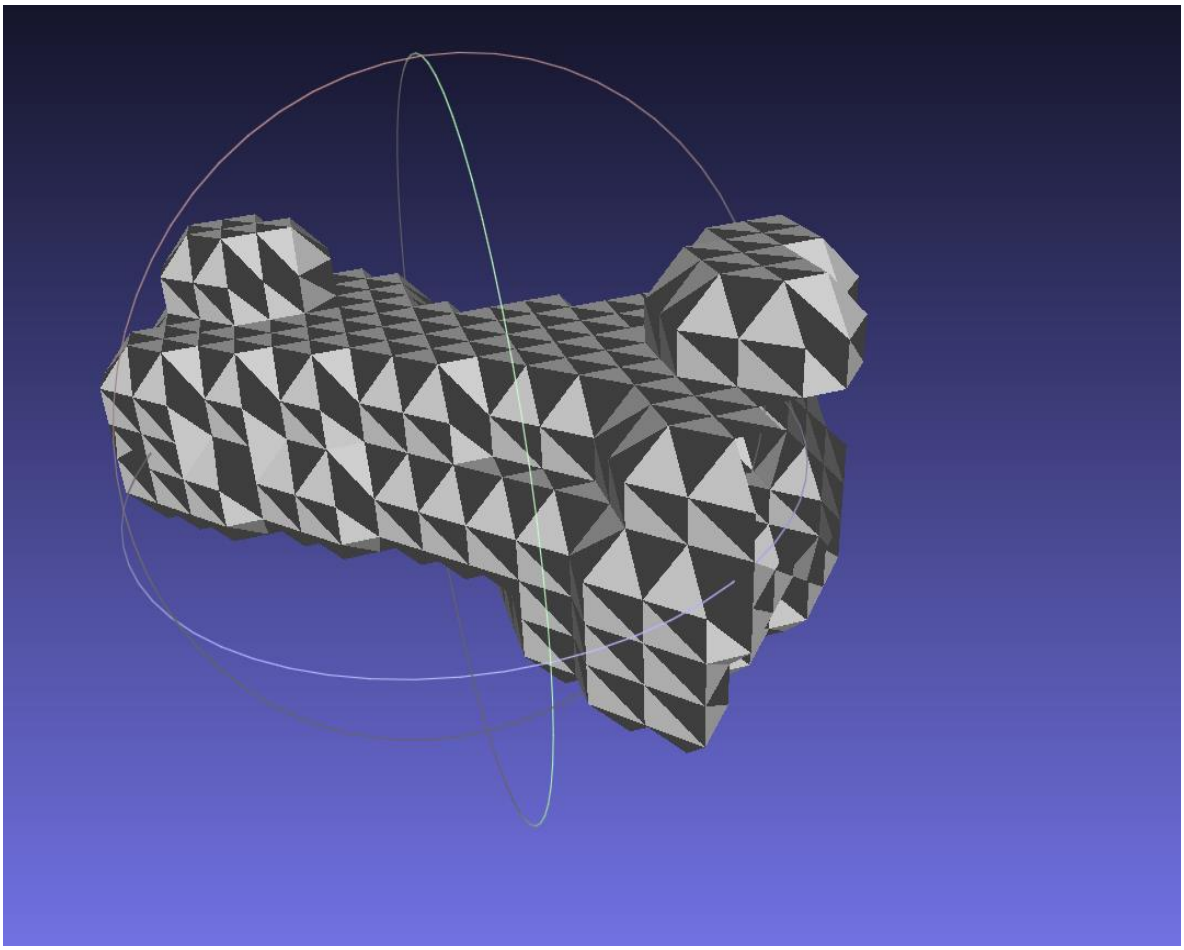

Figure 14. Right hand phalange distal 3 before normals are coherently re-oriented in Meshlab

Due to the fact that the faces are not oriented coherently, any attempts to repair the mesh further become more complicated and could even dramatically deform the shape of the mesh. To fix this issue within Meshlab, the re-orient all faces coherently tool is used. This causes all the normal planes of the triangular faces on the mesh to either face inward or outward as seen in Figure 15.

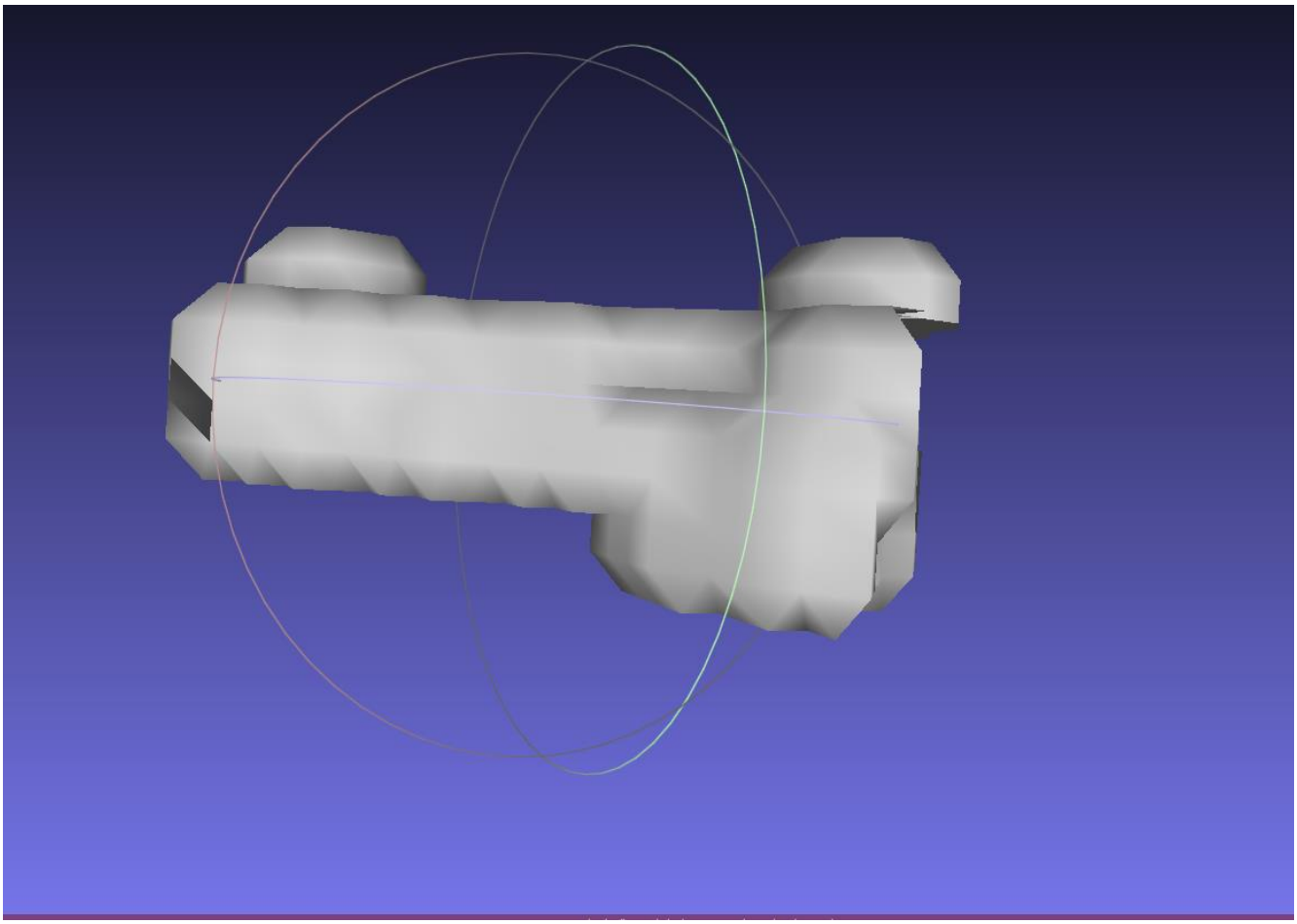

Figure 15. Right hand phalange distal 3 after normals are coherently re-oriented in Meshlab

Our ideal outcome is that all the face normals on the triangular faces are oriented coherently outward, but even if they are oriented coherently inward this is something that can be easily fixed in the next part of our workflow. The final thing that has to be done in this step is to export the altered model in the desired format.

Repairing, smoothing, and reducing triangle size

The next set of steps in the workflow are used to repair a model, smooth over the rough cubic edges, and reduce the number of triangles on the model while also increasing the triangular quality of each triangle in your mesh. These steps will be done using the mesh processing

software Meshmixer. Just as before, the process is started by importing the model you want to work on into Meshmixer. The first step is a continuation from the step prior to this one on the flow chart. If the normal plane of the triangular faces are coherently inward, they must be flipped outward. This is accomplished by selecting all the faces of your model in Meshmixer, then using the built-in select tools to flip the normal planes of the triangular faces outward. The before and after images of this process can be seen in Figures 16-17.

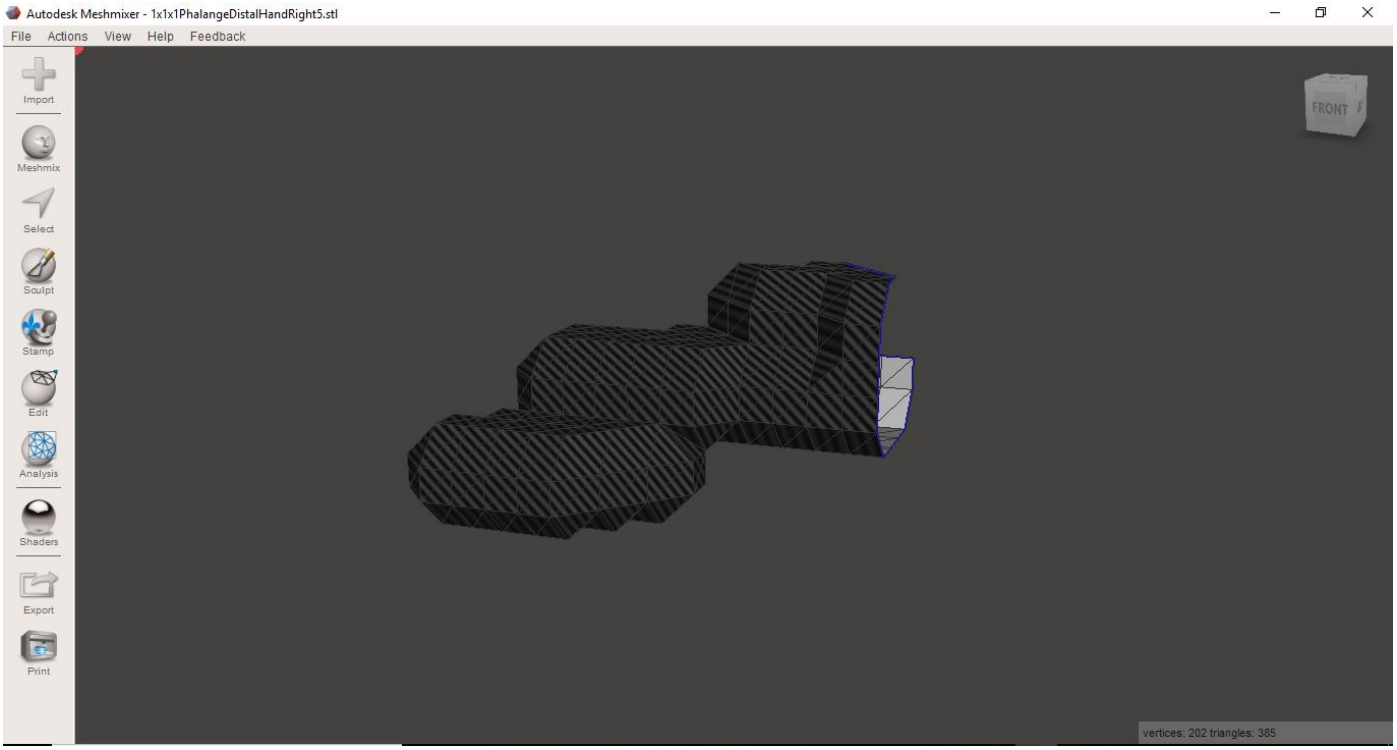

Figure 16. Right hand phalange distal 5 before normals are coherently re-oriented inward in Meshmixer

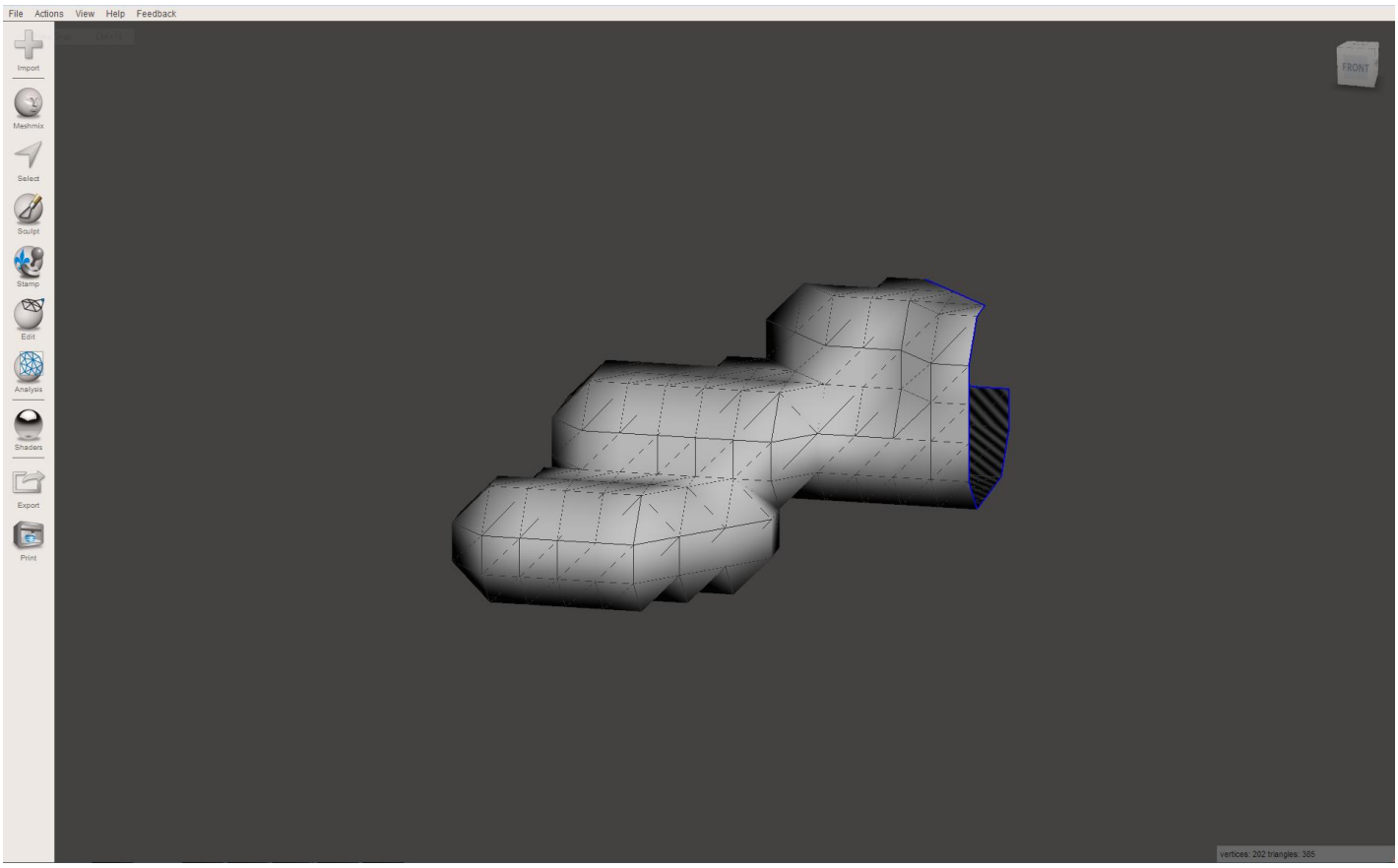

Figure 17. Right hand phalange distal 5 after normals are coherently flipped outward in Meshmixer

Once this is done and all the triangular faces of your models are facing outward, the next step is making your mesh watertight. A watertight mesh is one that has no holes anywhere on the surface of the mesh. Meshmixer has a built in analysis tool called inspector, which analyzes the model and looks for any holes, self-intersecting faces, or floating triangles within the mesh and highlights them as shown in Figure 18. Meshmixer color codes the highlighted regions depending on the problem found and proposed solution. Red highlights indicate non-manifold regions. Non-manifold elements are "bowtie" vertices or edges with more than two connected triangles. Blue highlights represent holes in the mesh. Magenta highlights indicate small-component areas.

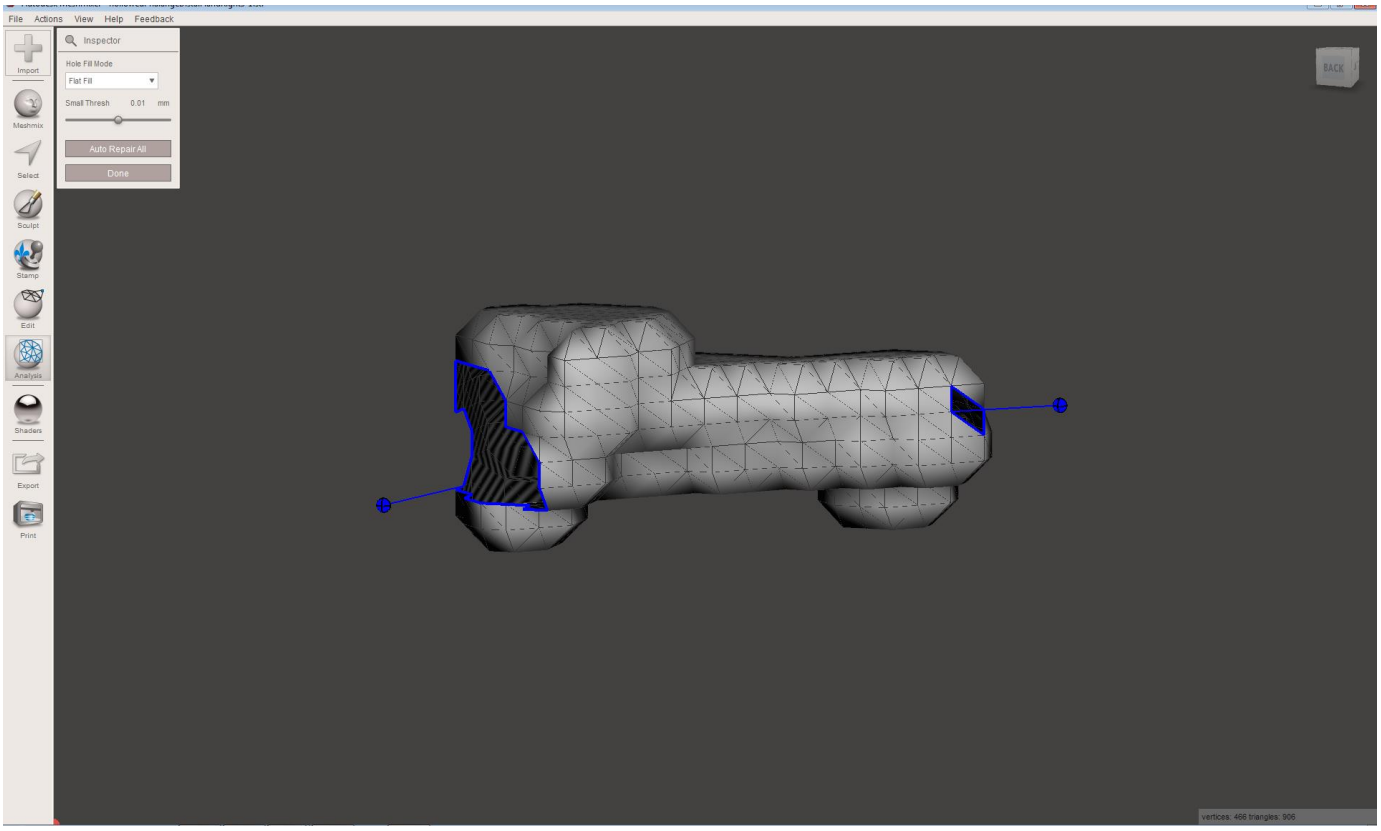

Figure 18. Right hand phalange distal 3 fixing holes with Meshmixer

Once the mesh is watertight the next step is to smooth over the rough sharp areas of the model. This is done by using the select tool in Meshmixer and selecting all the faces. Once the faces are selected, the deform tool is used to smooth the mesh. Figures 19 and 20 show the before and after images of this operation. When performing the smoothing operation, it is important to select shape preservation so that the model will not lose its shape.

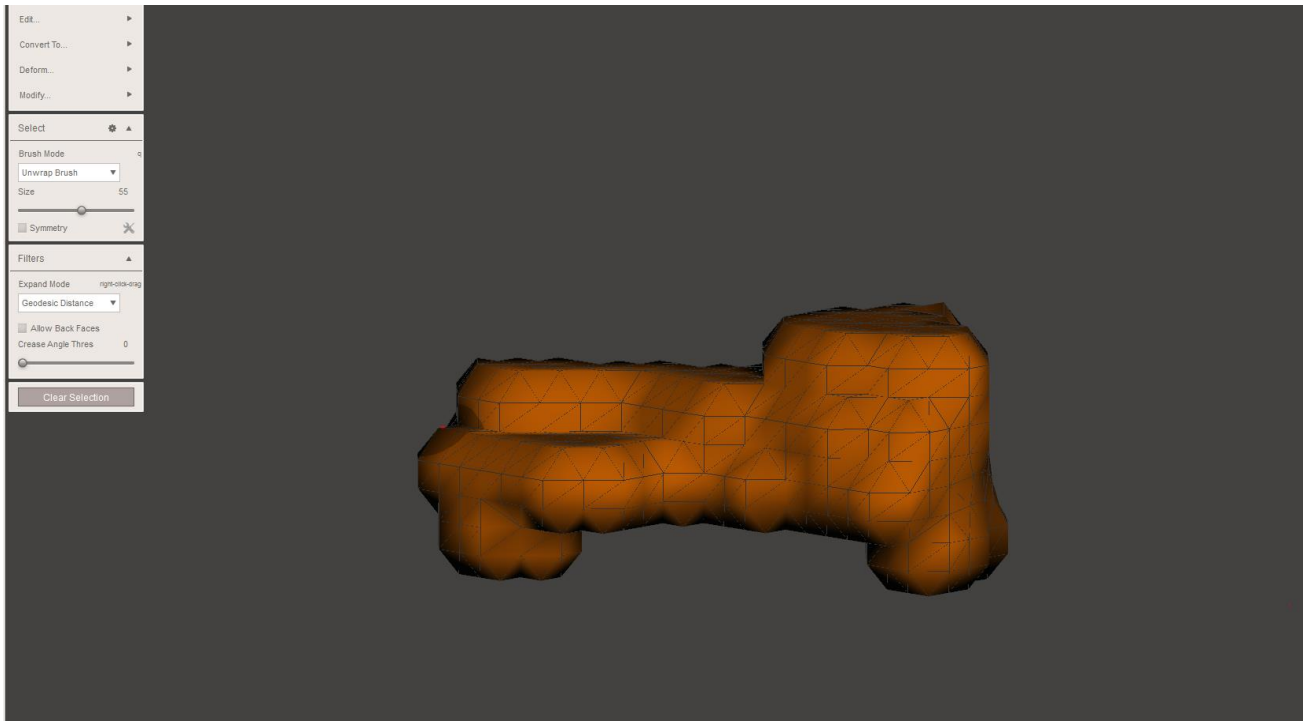

Figure 19. Prior to smoothing right hand phalange distal 3 mesh in Meshmixer

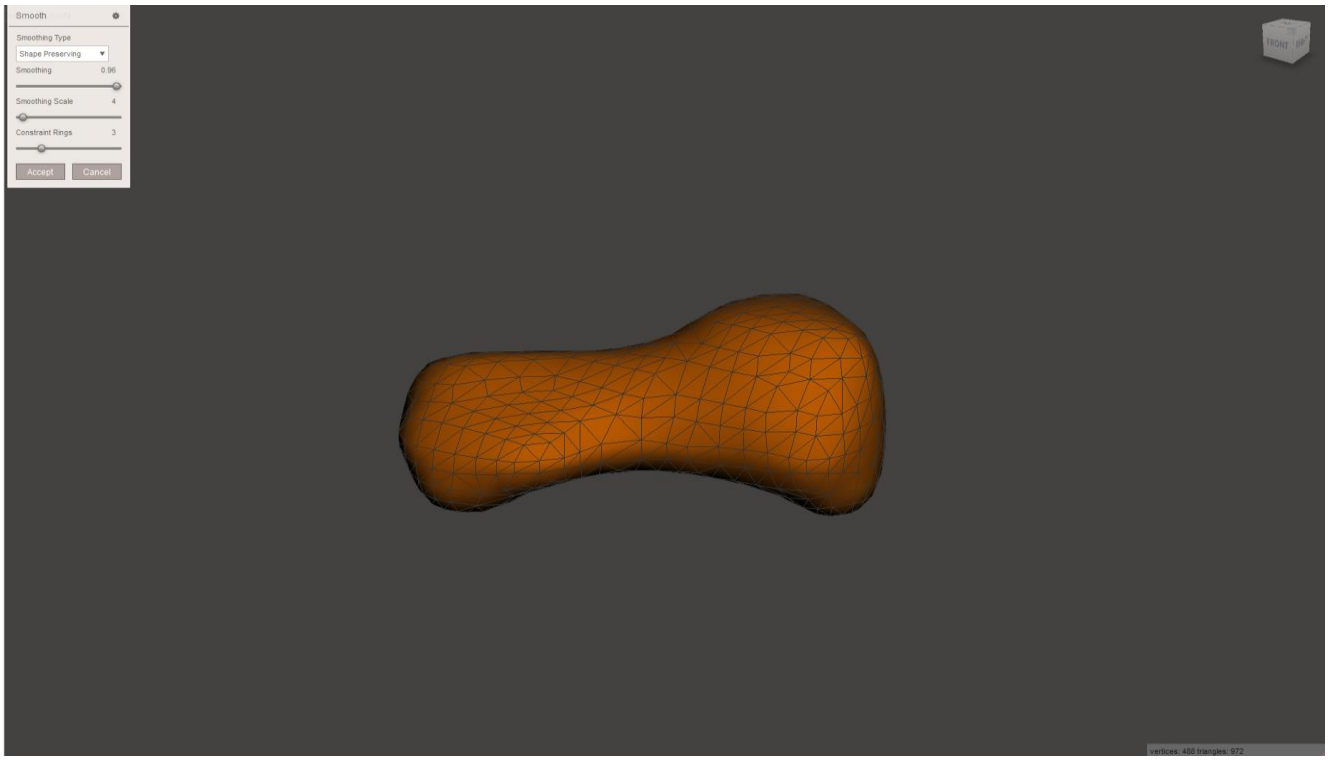

Figure 20. After smoothing right hand phalange distal 3 mesh in Meshmixer

After all rough edges have been smoothed, we must next reduce the number of triangles on our model while also increasing the quality of the triangles in the mesh. These two steps are interchangeable and at times need to be repeated. To reduce the number of triangles, once again select all the faces on your model in Meshmixer and use the edit tool to select reduce. The number of triangles may be reduced by a particular percentage, as shown in Figure 21. This is a very useful feature.

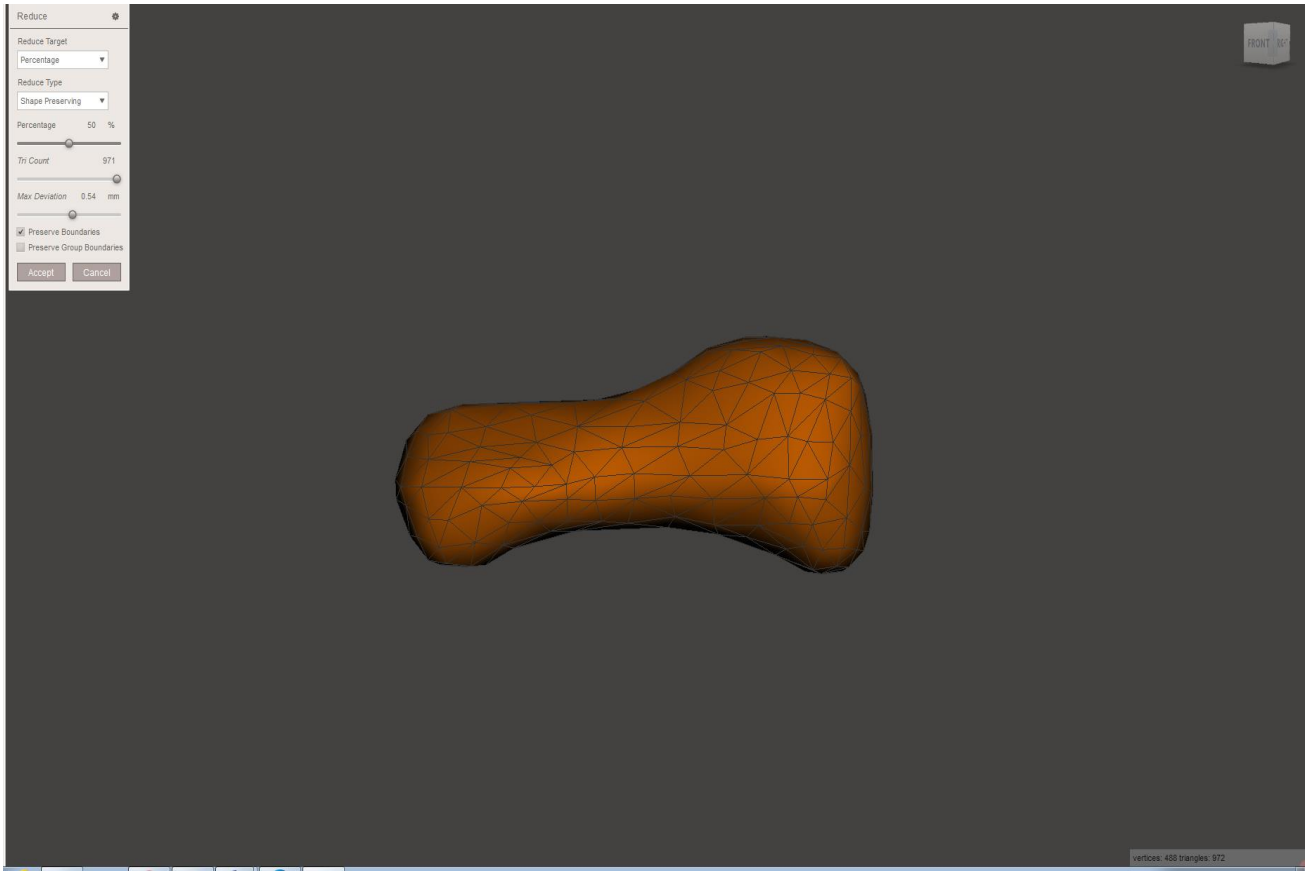

Figure 21. Reducing number of triangles on right hand phalange distal 3 mesh in Meshmixer

Once the number of triangles have been reduced, the next step is to use the remesh tool. The remesh tool allows you to retile a mesh with a new set of higher quality triangles throughout the mesh. The remesh tool provides a wide variety of customizability to ensure that a high

quality mesh is created without significantly increasing the number of triangles or losing the shape of the model. The remesh toolbar can be seen in Figure 22.

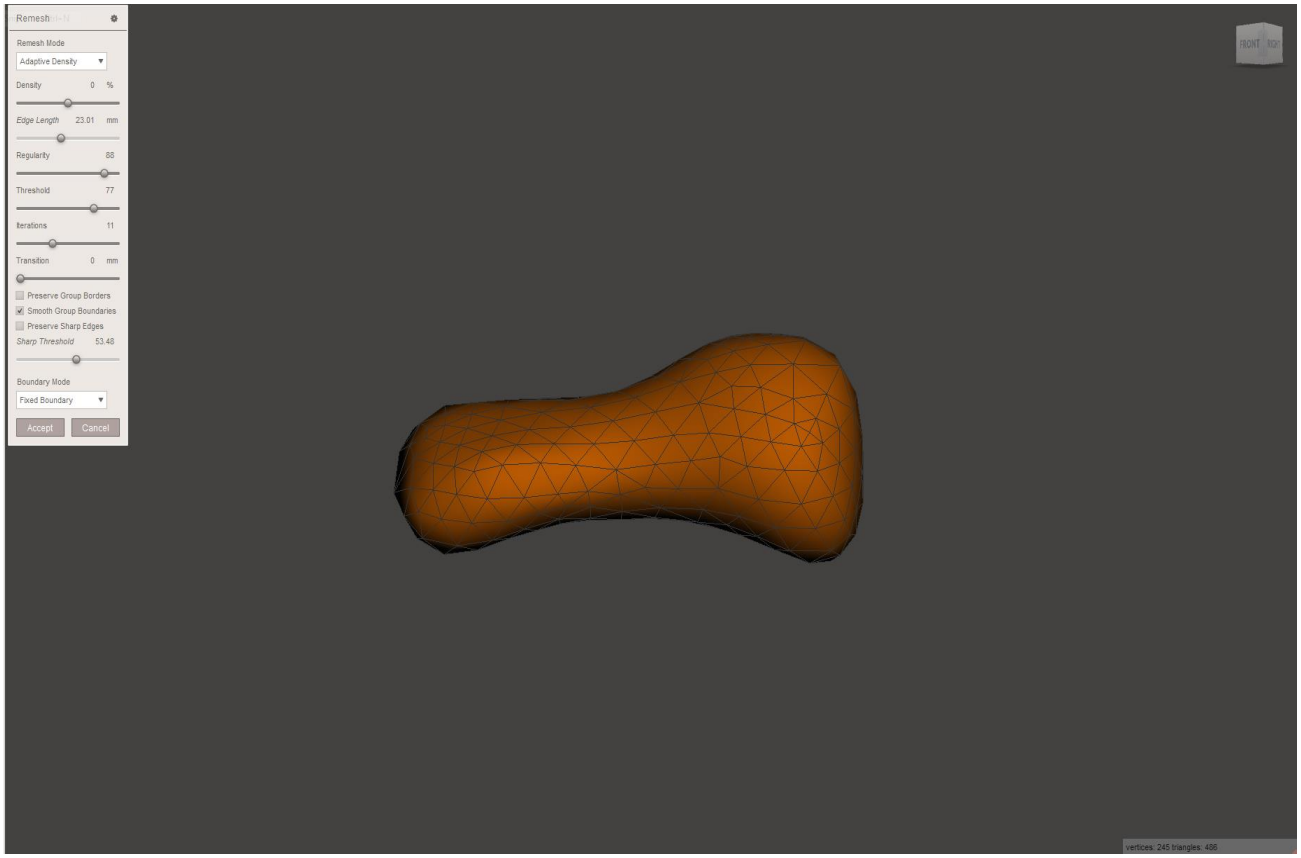

Figure 22. Remeshing triangular quality on right hand phalange distal 3 mesh in Meshmixer

The last step in the workflow is to double check the overall quality of the finished mesh model. This can be done in either Meshlab or MATLAB. Meshlab has a very convenient built in tool that color codes the quality of the triangles using the quality calculation discussed earlier in this paper, and provides a histogram of the quality of the triangles. The Meshlab quality analysis can be viewed in Figure 23.

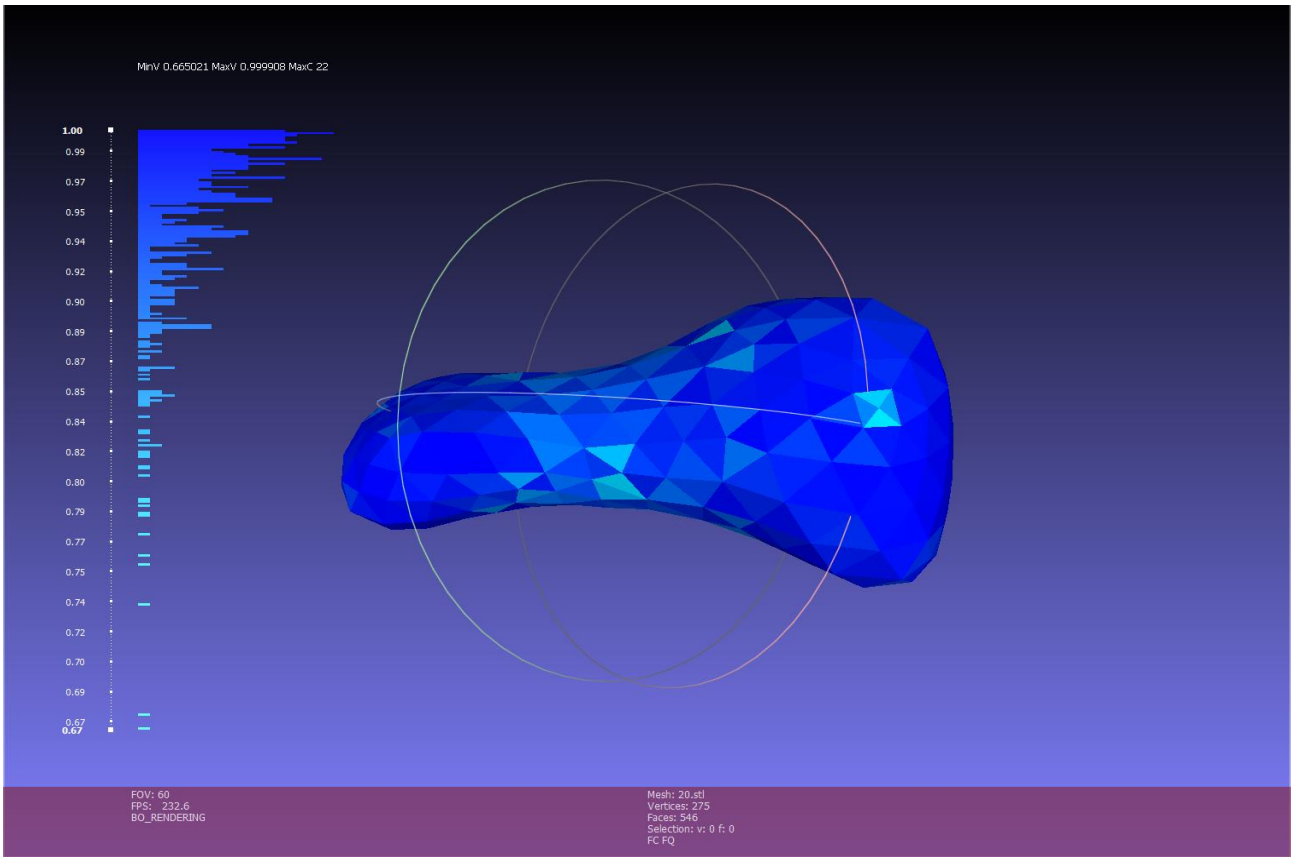

Figure 23. Quality histogram of triangles on right hand phalange distal 3 mesh in Meshlab

Some mesh processing tools will encode the exported model differently, which will change the file size. For example, when Meshmixer exports a file, its file size is dependent on the number of triangles in kilobytes. On the other hand, files exported from Meshlab are binary encoded, making the file size much smaller. The smaller the file size, the less amount of time it takes to read into any software and the less space it takes in memory. It is therefore recommended to always export from Meshlab as a final step due to this reason.

Resulting Model

The final VHP male model for this project consisted of 122 bone meshes that are composed of significantly less triangles but with a quality that is substantially better than the original voxel models. Compared to the original model, which had 125 bones, three of the voxel bones meshes where not able to be processed through this method and could not be completed properly. Figures 24-25 demonstrate the completed bone meshes. Table 1 provides of a list of all the bone meshes that were processed and identifies quality metrics of each mesh before and after the procedure.

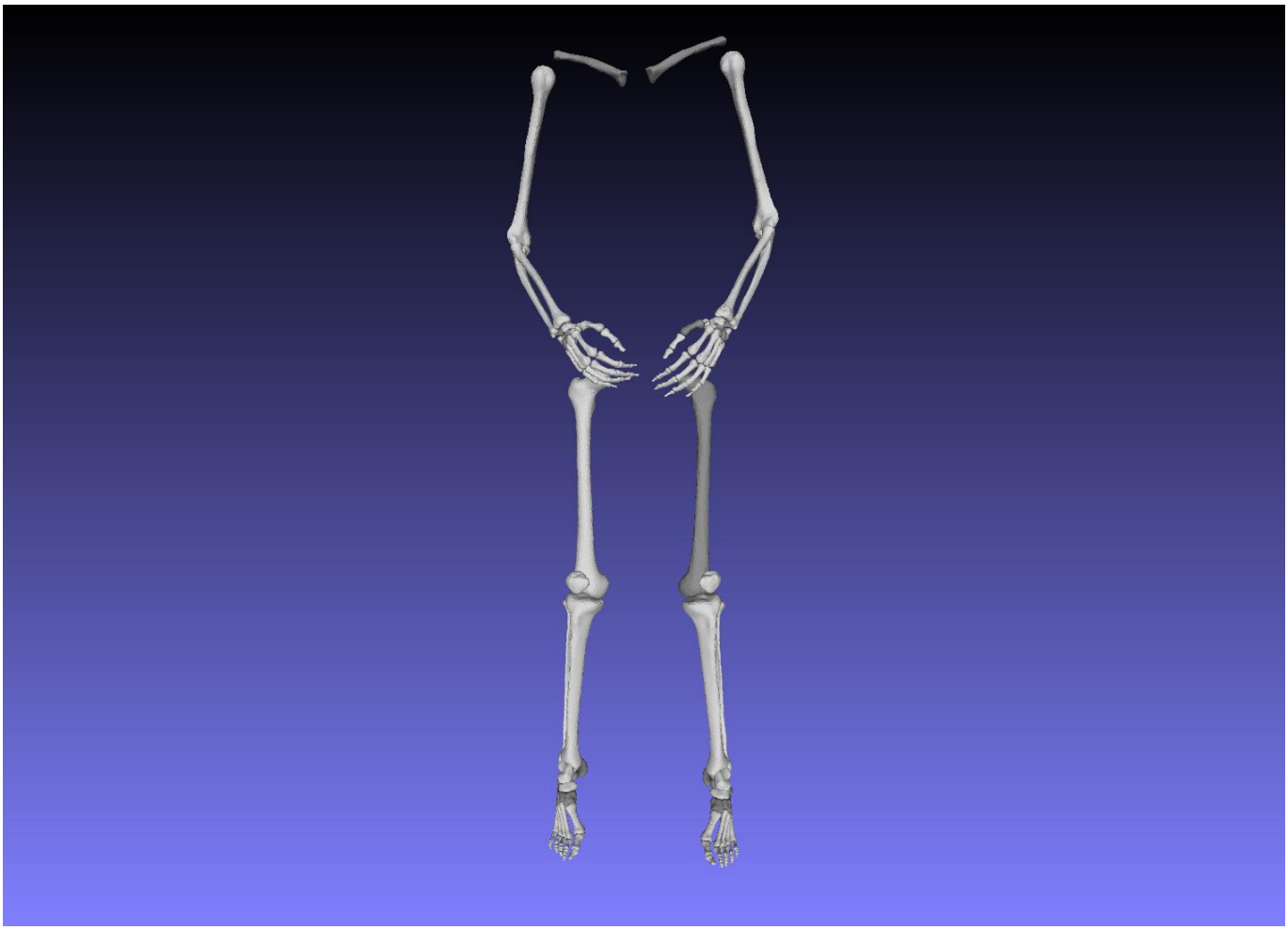

Figure 24. Final Smooth good quality Bone full bone mesh

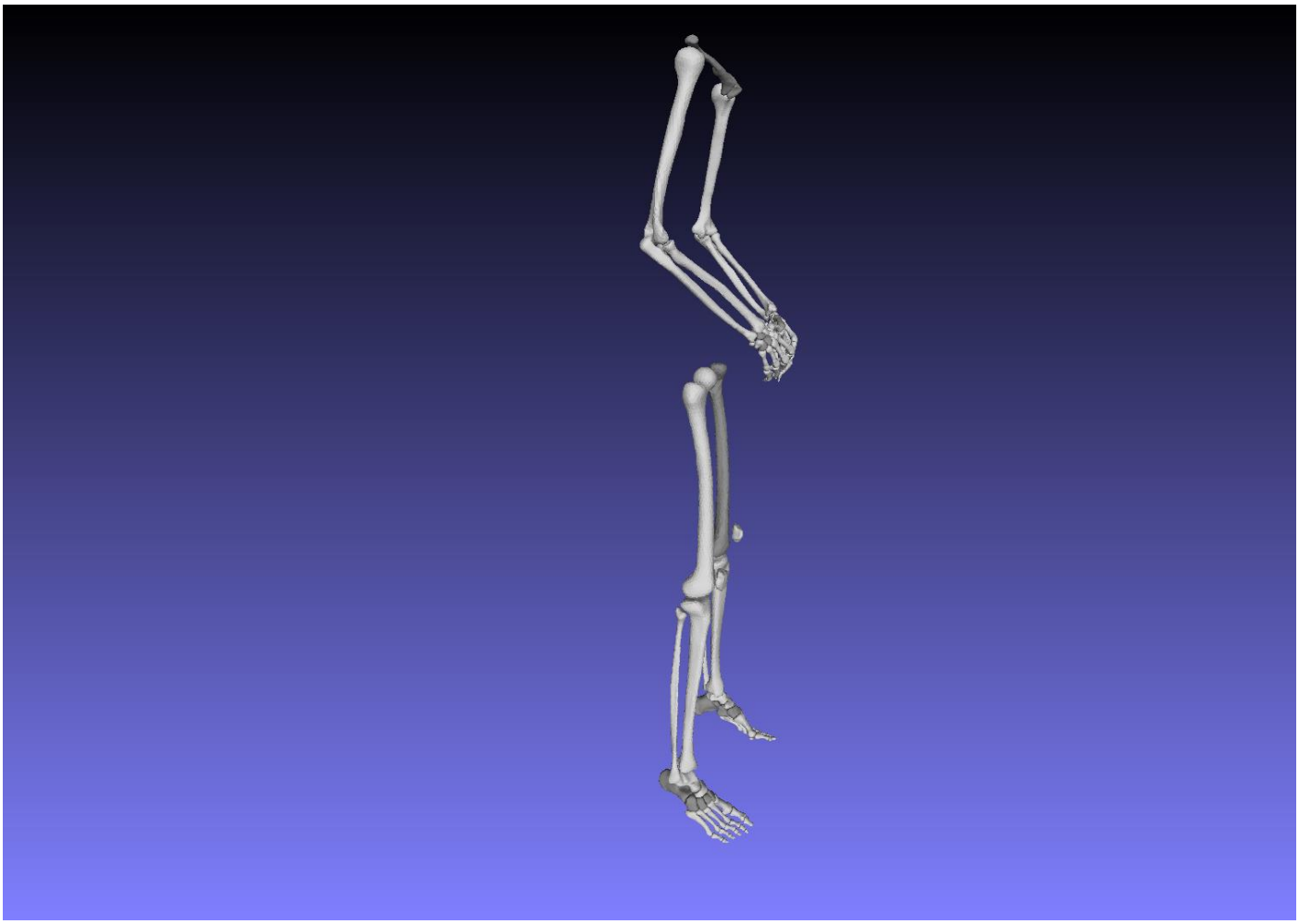

Figure 25. Side view of Final Smooth good quality Bone full bone mesh

Table 1. Processed VHP bone meshes with before and after quality data per bone

Bones	Number of triangles before	Number of Triangles after	Mesh quality before processing	Mesh quality after processing	Min Edge Length before	Min_Edge_ Length after
Calcaneus Left	36521	7964	0.78768	0.60953	0.99996	0.6512
Calcaneus Right	37732	9458	0.78769	0.60028	0.99999	0.72815
capitate left	2646	1406	0.78768	0.57285	0.99996	0.65252
capitate Right	2897	1338	0.78769	0.66788	1	0.59491
Clavicle Left	30236	6476	0.78768	0.62909	0.99996	0.67193
Clavicle Right	28868	9822	0.78769	0.56658	0.99998	0.55271

Bones	Number of triangles before	Number of Triangles after	Mesh quality before processing	Mesh quality after processing	Min Edge Length before	Min_Edge_ Length after
Cuboid Left	11633	2914	0.78768	0.65777	0.99996	0.82891
Cuboid Right	11465	2602	0.78769	0.73481	1	0.92239
Cuniform Intermediate Left	3831	1504	0.78768	0.67528	0.99996	0.65126
Cuniform Intermediate Right	3782	1184	0.78769	0.73695	1	0.92385
Cuniform Lateral Left	6528	1718	0.78768	0.69945	0.99996	0.76349
Cuniform Lateral Right	6195	1804	0.78769	0.72405	1	0.80658
Cuniform Medial Left	8288	2294	0.78768	0.67555	0.99996	0.58301
Cuniform Medial Right	8424	2334	0.78769	0.72702	1	0.91644
Femur Left	962	2786	0.03283	0.54446	2.62513	2.28329
Femur Right	240551	3034	0.78766	0.5629	0.99987	3.27147
Fibula Left	55512	4826	0.78767	0.5833	0.99996	1.2435
Fibula Right	54891	5442	0.78768	0.44894	0.99996	0.86787
Hamate Left	2483	1422	0.78768	0.61726	0.99996	0.70435
Hamate Right	2660	1552	0.78769	0.64537	1	0.68842
Humerus Left	111132	3634	0.78768	0.51261	0.99996	1.60986
Humerus Right	113138	1958	0.78769198	0.560239275	0.9999923706	1.975612763
Hyoid	3949		0.7876937002		1	
Lunate Left	1982	982	0.7876868191	0.7377956433	0.9999694824	0.7725618251
Lunate Right	2044	1206	0.78769	0.6152	1	0.50233
Metacarpal Left 1	4933	1826	0.78769	0.53085	1	0.47633
Metacarpal Left 2	5984	1090	0.78769	0.74763	1	1.27935
Metacarpal Left 3	5812	3116	0.78769	0.63368	1	0.61228
Metacarpal Left 4	4134	2112	0.78768	0.66014	0.99996	0.42923
Metacarpal Left 5	3578	1842	0.78768	0.55822	0.99996	0.66017
Metacarpal Right 1	5100	2642	0.78769	0.60166	0.99998	0.36416
Metacarpal Right 2	6312	3090	0.78769	0.6314	0.99998	0.73648
Metacarpal Right 3	5967	3186	0.78769	0.72341	0.99998	0.50038

Bones	Number of triangles before	Number of Triangles after	Mesh quality before processing	Mesh quality after processing	Min Edge Length before	Min_Edge_ Length after
Metacarpal Right 4	4248	1838	0.78769	0.6768	1	0.82814
Metacarpal Right 5	3693	1736	0.78766	0.58923	0.99987	0.66364
Metatarsal Left 1	14798	4284	0.78768	0.56538	0.99996	0.7403
Metatarsal Left 2	9258	2810	0.78768	0.74195	0.99996	0.77805
Metatarsal Left 3	8712	2778	0.78768	0.63547	0.99996	0.71483
Metatarsal Left 4	8355	2660	0.78769	0.65687	1	0.73853
Metatarsal Left 5	8958	2862	0.78769	0.55415	1	0.73383
Metatarsal Right 1	15585	4492	0.78769	0.50297	1	0.61599
Metatarsal Right 2	8819	2894	0.78769	0.58848	1	0.72677
Metatarsal Right 3	8477	2668	0.78769	0.61489	1	0.72417
Metatarsal Right 4	8318	2018	0.78769	0.71633	1	1.04424
Metatarsal Right 5	9465	2862	0.78769	0.64003	1	0.79194
Navicular Left	9511	1524	0.78768	0.6568	0.99996	0.92641
Navicular Right	8732	2140	0.78769	0.79963	1	0.91447
Patella Left	9256	2262	0.78768	0.69886	0.99996	0.92089
Patella Right	9582	2188	0.78769	0.72084	1	0.59574
Phalange Distal Foot Left 1	2343	1084	0.78769	0.70691	1	0.68197
Phalange Distal Foot Left 2	554	462	0.78768	0.67859	0.99996	0.5249
Phalange Distal Foot Left 3	674	390	0.78769	0.63465	1	0.64376
Phalange Distal Foot Left 4	521	422	0.78769	0.75935	1	0.65792
Phalange Distal Foot Left 5	379	380	0.78769	0.66388	1	0.37399
Phalange Distal Foot Right 1	2498	990	0.78769	0.69022	1	0.75296
Phalange Distal Foot Right 2	544	384	0.78769	0.78729	1	0.52908
Phalange Distal Foot Right 3	519	336	0.78769	0.66951	1	0.60779
Phalange Distal Foot Right 4	435	408	0.78769	0.59404	0.99998	0.43994
Phalange Distal Foot Right 5	329	310	0.78769	0.63478	1	0.52441

Bones	Number of triangles before	Number of Triangles after	Mesh quality before processing	Mesh quality after processing	Min Edge Length before	Min_Edge_ Length after
Phalange Distal Hand Left 1	***1431***	***922***	0.78769	0.6593	1	0.55001
Phalange Distal Hand Left 2	***859***	***526***	0.78767	0.5599	0.99993	0.64777
Phalange Distal Hand Left 3	***904***	***566***	0.78769	0.61224	1	0.55538
Phalange Distal HandLeft 4	***799***	***514***	0.78769	0.61903	1	0.49728
Phalange Distal Hand Left 5	***579***	***460***	0.78769	0.565	1	0.42676
Phalange Distal Hand Right 1	***1533***	***1062***	0.78769	0.68904	1	0.52193
Phalange Distal Hand Right 2	***641***	***708***	0.78769	0.73914	1	0.42212
Phalange Distal Hand Right 3	***906***	***634***	0.78766	0.6838	0.99987	0.49264
Phalange Distal Hand Right 4	***971***	***646***	0.78767	0.5517	0.99993	0.63482
Phalange Distal Hand Right 5	***385***	***476***	0.78769	0.53931	1	0.42394
Phalange Intermediate Foot Left 2	***1050***	***504***	0.78768	0.61546	0.99996	0.72336
Phalange Intermediate Foot Left 3	***852***	***420***	0.78769	0.72232	1	0.66644
Phalange Intermediate Foot Left 4	***683***	***444***	0.78769	0.66342	0.99998	0.68642
Phalange Intermediate Foot Left 5	***410***	***384***	0.78769	0.6444	1	0.39583
Phalange Intermediate Foot Right 2	***1040***	***498***	0.78769	0.71821	1	0.7816

Bones	Number of triangles before	Number of Triangles after	Mesh quality before processing	Mesh quality after processing	Min Edge Length before	Min_Edge_ Length after
Phalange Intermediate Foot Right 3	917	440	0.78769	0.7242	0.99998	0.61362
Phalange Intermediate Foot Right 4	579	380	0.78769	0.75065	1	0.63323
Phalange Intermediate Foot Right 5	368	398	0.78769	0.66206	1	0.65075
Phalange Intermediate Hand Left 2	1578	1074	0.78766	0.71188	0.99987	0.6843
Phalange Intermediate Hand Left 3	2304	1216	0.78767	0.60921	0.99993	0.53206
Phalange Intermediate Hand Left 4	1965	1198	0.78769	0.71882	1	0.58757
Phalange Intermediate Hand Left 5	1241	724	0.78769	0.6388	1	0.73766
Phalange Intermediate Hand Right 2	1677	964	0.78769	0.68893	1	0.62334
Phalange Intermediate Hand Right 3	2032	1254	0.78766	0.50546	0.99987	0.37928
Phalange Intermediate Hand Right 4	1926	1054	0.78767	0.64528	0.99993	0.60424
Phalange Intermediate Hand Right 5	1661	896	0.78769	0.61887	1	0.71825
Phalange Proximal Foot Left 1	4832	1792	0.78769	0.6381	0.99998	0.60141
Phalange Proximal Foot Left 2	2373	1010	0.78768	0.64819	0.99996	0.64416

Bones	Number of triangles before	Number of Triangles after	Mesh quality before processing	Mesh quality after processing	Min Edge Length before	Min_Edge_ Length after
Phalange Proximal Foot Left 3	***2200***	***868***	0.78768	0.72881	0.99996	0.67317
Phalange Proximal Foot Left 4	***2184***	***884***	0.78769	0.57002	0.99998	0.58089
Phalange Proximal Foot Left 5	***2044***	***906***	0.78769	0.64608	1	0.68297
Phalange Proximal Foot Right 1	***5589***	***1774***	0.78769	0.70863	0.99998	0.81973
Phalange Proximal Foot Right 2	***2444***	***946***	0.78769	0.516	0.99998	0.71409
Phalange Proximal Foot Right 3	***2196***	***880***	0.78769	0.69603	0.99998	0.59066
Phalange Proximal Foot Right 4	***1907***	***830***	0.78769	0.82573	1	0.77002
Phalange Proximal Foot Right 5	***2040***	***980***	0.78769	0.57721	1	0.45732
Phalange Proximal Hand Left 1	***2671***	***1304***	0.78769	0.53321	1	0.65891
Phalange Proximal Hand Left 2	***3367***	***1624***	0.78766	0.7234	0.99987	0.75341
Phalange Proximal Hand Left 3	***3814***	***1922***	0.78766	0.58247	0.99987	0.57153
Phalange Proximal Hand Left 4	***3360***	***1704***	0.78766	0.64734	0.99987	0.7696
Phalange Proximal Hand Left 5	***2224***	***1178***	0.78766	0.63196	0.99987	0.76114
Phalange Proximal Hand Right 1	***2909***	***1416***	0.78769	0.71736	1	0.58432
Phalange Proximal Hand Right 2	***3684***	***1912***	0.78769	0.57698	1	0.49732
Phalange Proximal Hand Right 3	***4281***	***2234***	0.78766	0.61623	0.99987	0.60361
Phalange Proximal Hand Right 4	***3383***	***1622***	0.78766	0.53018	0.99987	0.58124
Phalange Proximal Hand Right 5	***2341***	***1316***	0.78766	0.57449	0.99987	0.50285

Bones	Number of triangles before	Number of Triangles after	Mesh quality before processing	Mesh quality after processing	Min Edge Length before	Min_Edge_ Length after
Pisiform Left	1178	814	0.78768	0.72795	0.99996	0.62712
Pisiform Right	1128	594	0.78769	0.83891	1	0.83038
Radius Left	45310	3570	0.78768	0.63188	0.99996	1.36156
Radius Right	46851	2960	0.78769	0.57984	0.99998	0.81152
Scaphoid Left	2767	1604	0.78768	0.68197	0.99996	0.41313
Scaphoid Right	2735	1338	0.78769	0.79458	1	0.69027
Scapula Left	114577		0.78768		0.99996	0
Scapula Right	115151		0.78768		0.99998	0
Talus Left	24247	2208	0.78768	0.56792	0.99996	1.35334
Talus Right	24259	1872	0.78769	0.69936	0.99999	1.10178
Tibia Left	161280	2924	0.78768	0.53085	0.99996	1.78525
Tibia Right	164669	2934	0.78768	0.59517	0.99996	2.56285
Trapezium Left	2167	1148	0.78769	0.68801	1	0.66998
Trapezium Right	2096	1088	0.78769	0.6359	1	0.50822
Trapezoid Left	1213	896	0.78769	0.73282	1	0.71879
Trapezoid Right	1346	928	0.78769	0.6041	1	0.67904
Triquetral Left	2153	1218	0.78768	0.59704	0.99996	0.49695
Triquetral Right	1831	1088	0.78769	0.6311	1	0.74665
Ulna Left	50501	4138	0.38145	0.54022	0.58729	0.96972
Ulna Right	51099	4286	0.78769	0.61489	1	0.72417

In addition to the bone meshes described above, several different meshes were processed in hopes to increase the triangular mesh quality for a commercial customer, Bose. The same workflow was used when processing these meshes. Table 2 displays the top 10 percent of the worst quality triangles before and after processing of the meshes, along with the number of triangles. Figures 26-27 are visual graphs which demonstrate the change in mesh quality before and after processing.

Table 2. Processed Bose meshes with before and after quality data per mesh

Before quality		Number of Triangles		After Quality		Number of Triangles	
Skin	fat	before skin	before fat	Skin	Fat	After Skin	after fat
0.000476	0.000008	14608	15050	0.070670	0.014609	10666	12370
0.001495	0.000013			0.078419	0.120076		
0.003102	0.000016			0.082675	0.183569		
0.003288	0.0021572			0.086103	0.222168		
0.003358	0.0055231			0.101883	0.224617		
0.003799	0.008388			0.111397	0.272219		
0.003822	0.008442			0.120994	0.274374		
0.004054	0.012719			0.121562	0.293857		
0.009370	0.014455			0.122916	0.301208		
0.015890	0.016513			0.125612	0.304179		
0.017766	0.020346			0.133014	0.330349		
0.018716	0.020725			0.137569	0.343346		
0.019060	0.026197			0.168689	0.351027		
0.020783	0.027453			0.210730	0.353483		
0.024402	0.028005			0.227419	0.354121		
0.024783	0.028230			0.230247	0.357707		
0.025310	0.028701			0.233014	0.357828		
0.026854	0.029270			0.237212	0.358918		
0.027122	0.029469			0.254983	0.359198		
0.027442	0.029671			0.255581	0.360112		
0.028405	0.030160			0.266480	0.368485		
0.031446	0.034243			0.278489	0.372200		
0.032946	0.034910			0.278887	0.376877		
0.033066	0.036512			0.287230	0.377615		
0.033478	0.037504			0.289240	0.382697		
0.035429	0.037642			0.298451	0.385500		
0.035901	0.038404			0.302831	0.387557		
0.036058	0.038800			0.304309	0.401078		
0.036177	0.040576			0.304840	0.408225		
0.036537	0.041126			0.310561	0.410629		
0.037706	0.04129			0.311105	0.414966		
0.038704	0.041392			0.319280	0.421862		
0.039422	0.041503			0.322224	0.423347		
0.041296	0.041955			0.324106	0.429967		
0.042410	0.0421390			0.331055	0.432639		

Before quality		Number of Triangles		After Quality		Number of Triangles	
Skin	fat	before skin	before fat	Skin	Fat	After Skin	after fat
0.043139	0.0425192			0.336040	0.445387		
0.043735	0.0431789			0.337029	0.446149		
0.044322	0.044454			0.346903	0.453531		
0.050151	0.0468791			0.34879	0.456606		
0.053117	0.0469761			0.35773	0.456623		
0.054116	0.0481895			0.366351	0.459555		
0.054284	0.0487692			0.370446	0.464525		
0.056118	0.0491538			0.370652	0.474046		
0.057240	0.0499695			0.370725	0.475913		
0.058340	0.0510840			0.372942	0.476774		
0.060487	0.0520606			0.381854	0.476984		
0.063486	0.0522083			0.384201	0.482835		
0.063891	0.0523288			0.384477	0.485299		
0.064737	0.0528583			0.387154	0.486912		
0.065778	0.0539398			0.394934	0.489348		
0.066694	0.0556976			0.401512	0.492776		
0.068885	0.0568326			0.402984	0.496390		
0.071422	0.0573621			0.411548	0.500375		
0.071909	0.0575055			0.411647	0.500676		
0.074189	0.0577931			0.414902	0.501919		
0.074260	0.0581266			0.428289	0.505175		
0.075436	0.0589671			0.433250	0.507043		
0.076802	0.0594308			0.437629	0.518176		
0.077419	0.0600513			0.438472	0.518749		
0.077455	0.0615756			0.444897	0.518756		
0.077648	0.0622579			0.445516	0.520115		
0.078664	0.0636961			0.448148	0.524265		
0.078780	0.0653742			0.448736	0.527110		
0.078857	0.0682015			0.449295	0.528231		
0.081386	0.0687440			0.45276	0.528240		
0.081529	0.070404			0.45772	0.531280		
0.081758	0.070562			0.46050	0.534707		
0.081873	0.072023			0.460729	0.534844		
0.082471	0.072628			0.468147	0.540736		
0.083040	0.075168			0.468799	0.5415635		
0.083212	0.0754802			0.471616	0.5432398		

Before quality		Number of Triangles		After Quality		Number of Triangles	
Skin	fat	before skin	before fat	Skin	Fat	After Skin	after fat
0.083912	0.0758278			0.472086	0.5447988		
0.084889	0.0762131			0.473847	0.547256		
0.084910	0.076517			0.473876	0.549123		
0.085394	0.0772273			0.480118	0.549797		
0.086255	0.0784427			0.484392	0.552436		
0.086557	0.0786145			0.484674	0.556200		
0.086807	0.0788824			0.487316	0.558081		
0.089844	0.0797553			0.488817	0.560664		
0.090394	0.0797669			0.490617	0.564268		
0.090486	0.0801667			0.501416	0.564370		
0.093265	0.0803250			0.503291	0.565339		
0.093306	0.0811941			0.507639	0.565760		
0.094577	0.0817732			0.507785	0.567007		
0.095136	0.0817760			0.510666	0.567158		
0.095140	0.0819405			0.511088	0.568412		
0.095777	0.0831301			0.513264	0.569070		
0.096028	0.0833053			0.514946	0.570955		
0.097296	0.0835276			0.515039	0.573085		
0.099656	0.0839064			0.516785	0.573830		

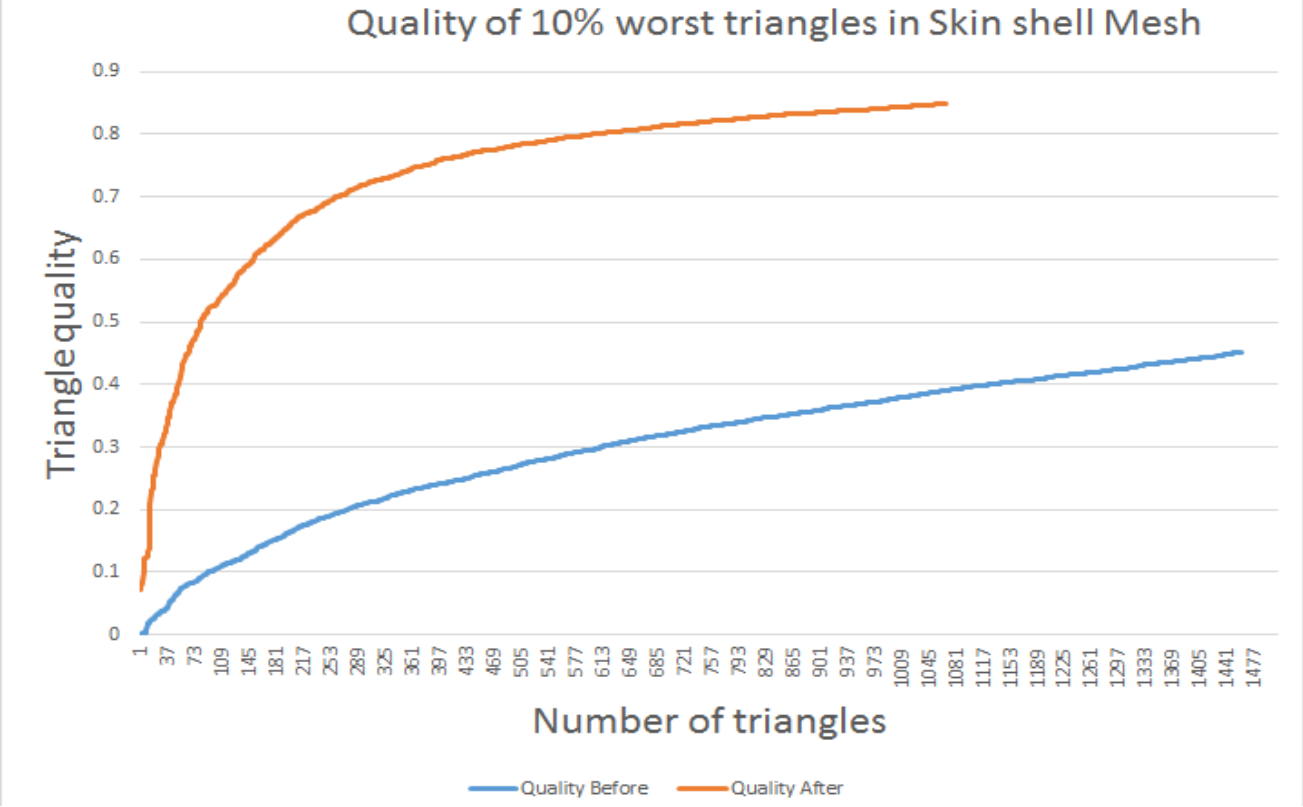

Figure 26. Triangular quality plot for the Bose Skin shell before and after mesh processing.

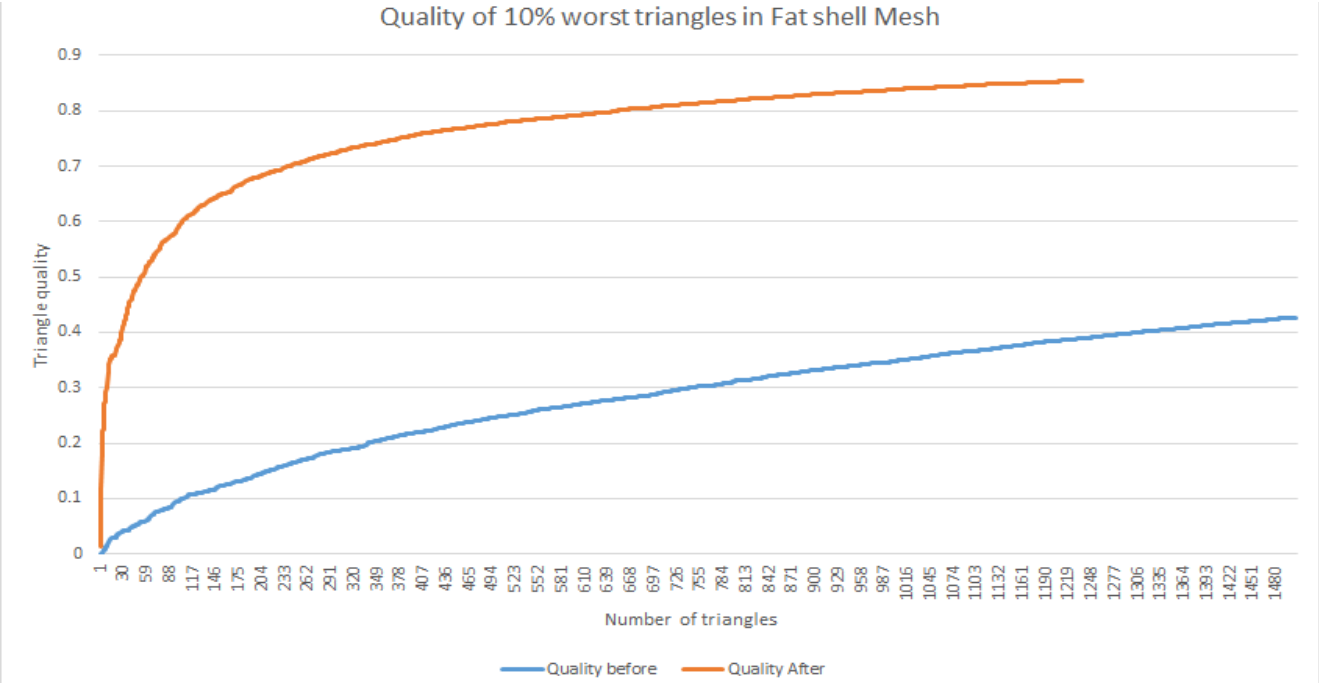

Figure 27. Triangular quality plot for the Bose Fat shell before and after mesh processing.

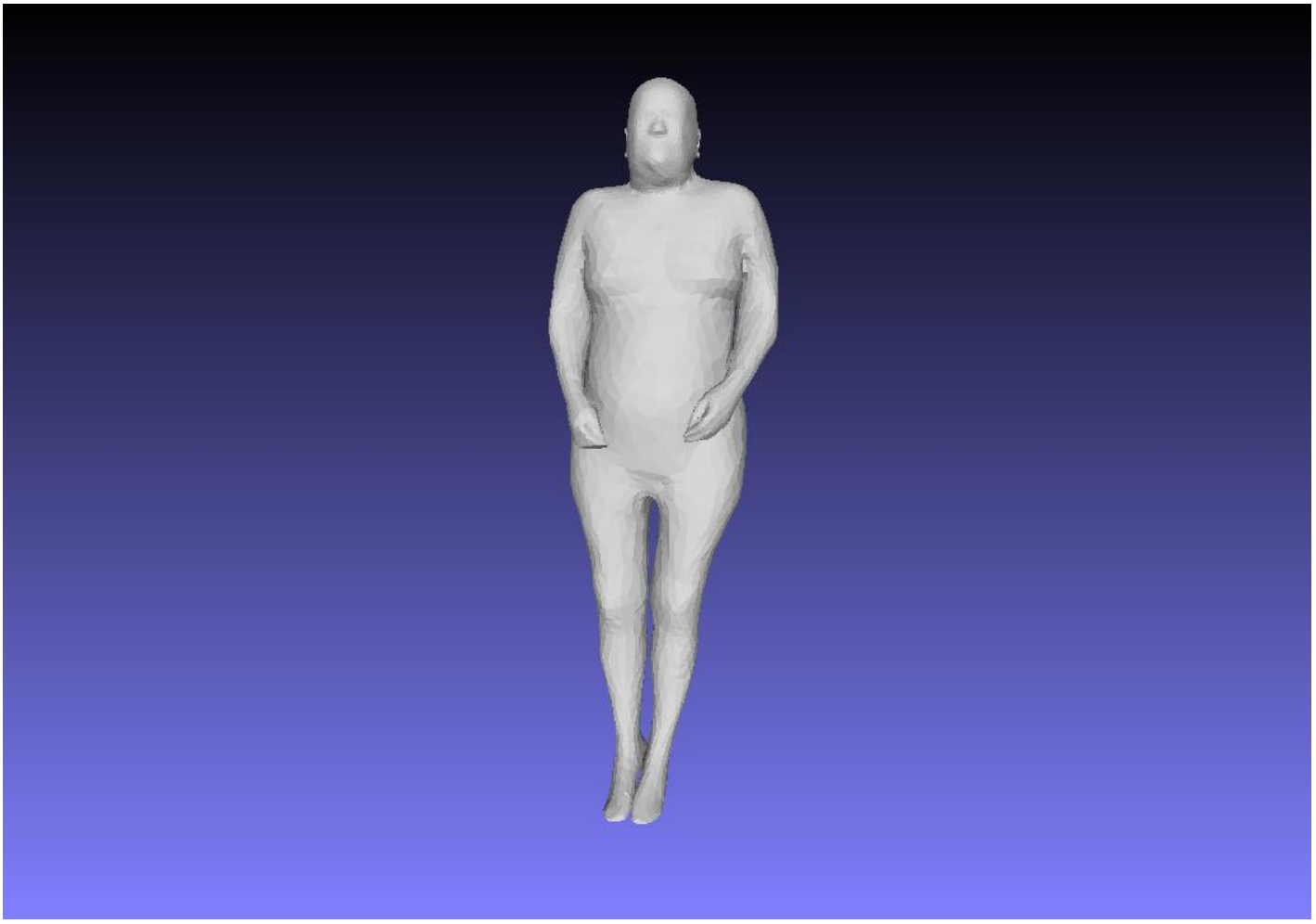

Figure 28 Quality Histogram in Meshlab of Bose Fat shell Mesh after Processing

Figures 29-32 show the quality histograms of the BOSE shell meshes before and after being processed in Meshlab.

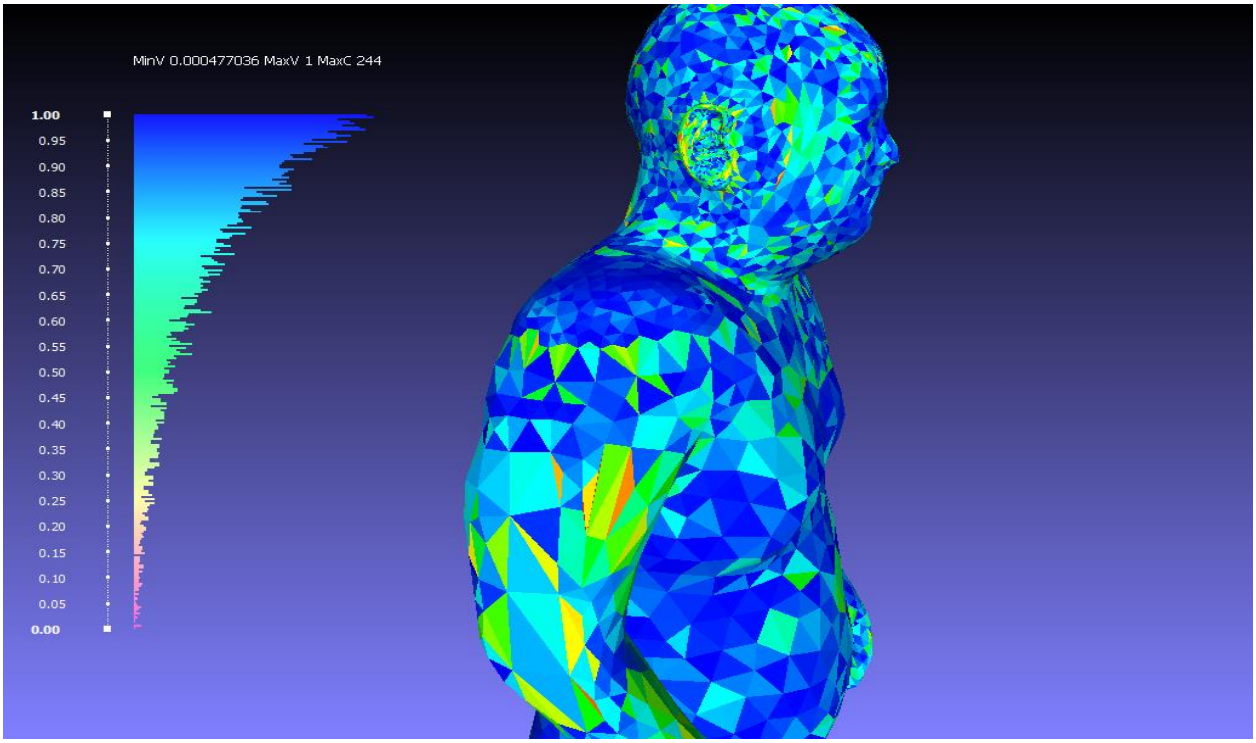

Figure 29. Quality Histogram in Meshlab of Bose Fat shell Mesh before Processing

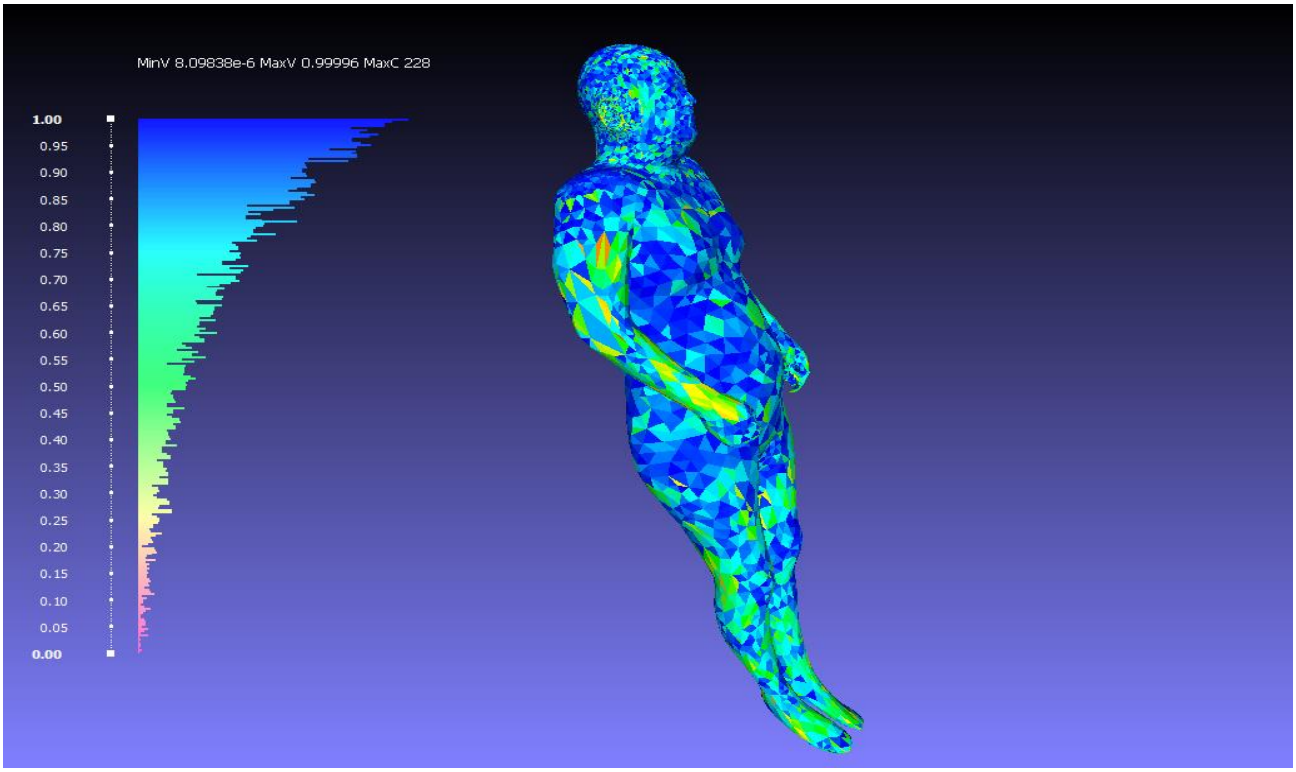

Figure 30. Quality Histogram in Meshlab of Bose Fat shell Mesh before Processing

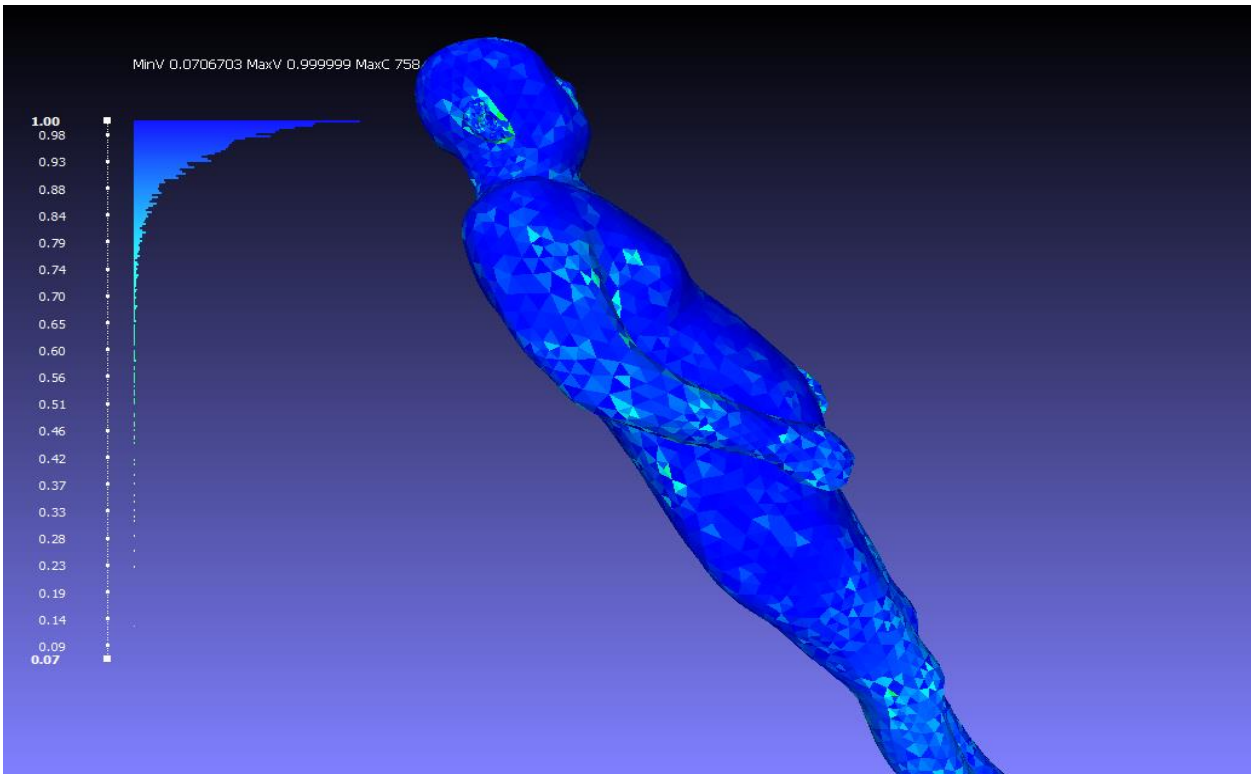

Figure 31. Quality Histogram in Meshlab of Bose Skin shell Mesh after Processing

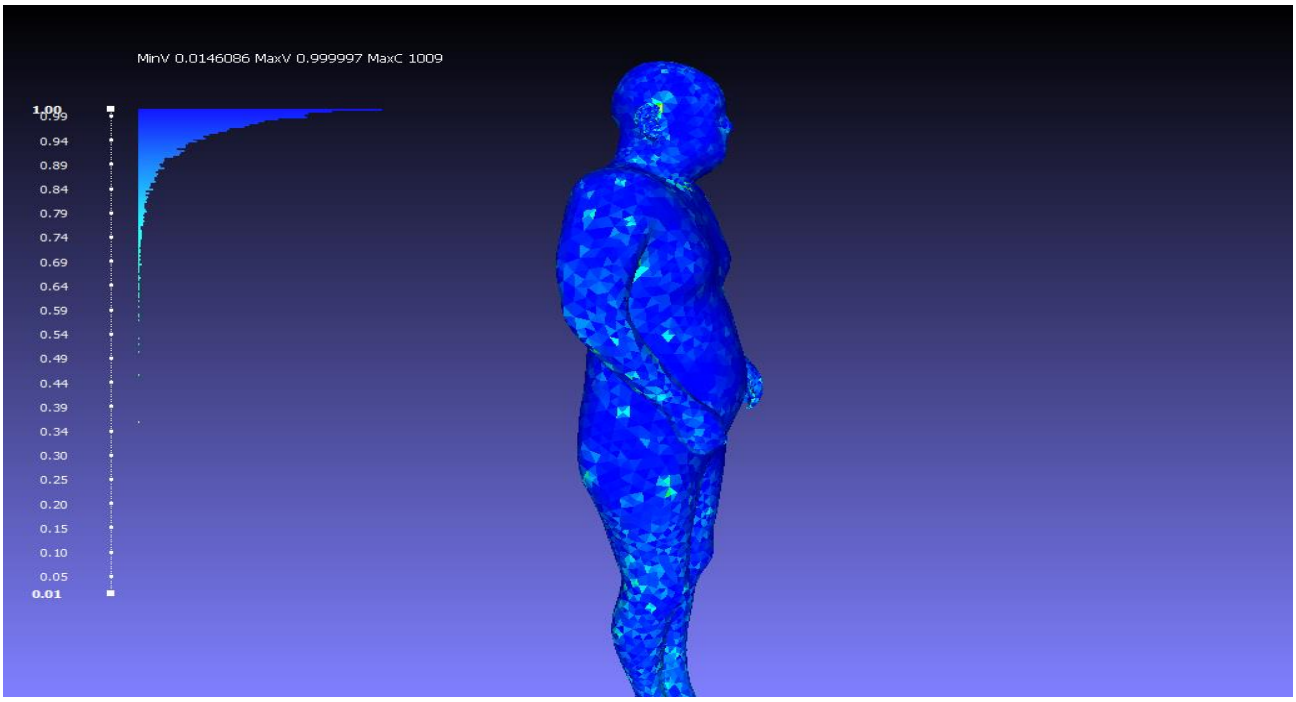

Figure 32 .Quality Histogram in Meshlab of Bose Fat shell Mesh after Processing

Future work

The next step in the project is to continue processing the remaining bone meshes to have a complete VHP Male skeleton. The created workflow should continue to be implemented to assure that the highest quality triangular meshes are created. Once the bones are completed, the next step is to process any additional meshes (i.e., soft tissues) that are necessary to create an anatomically correct VHP Male model. Once all meshes meet the requirements necessary of a good quality mesh, then computational analysis can be performed using the meshes.

Conclusion

The purpose of this MQP was to figure out a way to create high quality triangular surface meshes from voxel-based models that could be used for FEM analysis. In the process, a workflow was developed which uses multiple mesh processing software applications to accomplish the end goal. Over the length of this project, 122 VHP male bone meshes where processed together with two BOSE shell meshes. The resulting meshes were of very high quality and retained their original shape while significantly lowering the overall number of triangles. The results from this project will be used to continue the development of the model in the future Major Qualifying Projects at WPI. The meshes developed during this project will also be later used in verify the accuracy of the model and the final model will used in simulations with MRI coils.

References

[1] M.J. Ackerman, “The Visible Human Project®: From Body to Bits,” 38th Annual Int. Conf. of the IEEE Engineering in Medicine and Biology Society, Orlando, FL, Aug. 16-21, 2016.

[2] The Visible Human Project, U.S. National Library of Medicine. Available: https://www.nlm.nih.gov/research/visible/getting_data.html

[3] National Institute of Biomedical Imaging and Bioengineering, NIH: “Computational Modeling,” Sept. 2016. Available:

[4] https://www.nibib.nih.gov/science-education/science-topics/computational-modeling

[5] S.N. Makarov, G. M. Noetscher, J. Yanamadala, M. W. Piazza, S. Louie, A. Prokop, A. Nazarian, and A. Nummenmaa, “Virtual Humans Models for Electromagnetic Studies and Their Applications,” December 21, 2016.

[6] Makarov, S. N., Noetscher, G. M., & Nazarian, A. (2015). *Low-frequency electromagnetic modeling for electrical and biological systems using MATLAB*. John Wiley & Sons.

[7] Maino, Nicholas Daniel Student author -- ECE, Lacroix, Patrick Alphonse Student author -- ECE, & Makarov, Sergey N. Faculty advisor -- EE. (2017). *CAD virtual human male model*. Worcester, MA: Worcester Polytechnic Institute.

[8] L. Science, "Digital AustinMan Created to Study Cell Phone Radiation," *Live Science*, 2017. [Online]. Available: http://www.livescience.com/19554-austin-man-radiation-nsf-bts.html.